Earth Syst. Sci. Data Discuss., https://doi.org/10.5194/essd-2017-64
Manuscript under review for journal Earth Syst. Sci. Data
Discussion started: 28 August 2017

Open Access Earth System Science Data Discussions

Evaluation of *seNorge2*, a conventional climatological datasets for snow- and hydrological modeling in Norway

Cristian Lussana[1], Tuomo Saloranta[2], Thomas Skaugen[2], Jan Magnusson[2], Ole Einar Tveito[1], and Jess Andersen[2]

[1]Norwegian Meteorological Institute, Oslo, Norway
[2]Norwegian Water Resources and Energy Directorate, Oslo, Norway

Correspondence to: Cristian Lussana (cristianl@met.no)

Abstract. The conventional climate datasets based on observations only are a widely used source of information for climate and hydrology. On the Norwegian mainland, the seNorge datasets of daily mean temperature and total precipitation amount constitute a valuable meteorological input for snow- and hydrological simulations which are routinely conducted over such a complex and heterogeneous terrain. A new seNorge version (seNorge2) has been released recently and to support operational applications for civil protection purposes, it must be updated daily and presented on a high-resolution grid (1 Km of grid spacing). The archive goes back to 1957. The seNorge2 statistical interpolation schemes can provide high-resolution fields for applications requiring long-term datasets at regional or national level, where the challenge is to simulate small-scale processes often taking place in complex terrain. The statistical schemes build upon classical spatial interpolation methods, such as Optimal Interpolation and successive-correction schemes, and introduce original approaches. For both temperature and precipitation, the spatial interpolation exploits the concept of (spatial) scale-separation and the first-guess field is derived from the observed data. Furthermore, the geographical coordinates and the elevation are used as complementary information. The evaluation of the seNorge2 products is presented both from a general point of view, through systematic cross-validations, and specifically as the meteorological input in the operational model chains used for snow- and hydrological simulations. The seNorge snow model is used for simulation of snow fields and the DDD (Distance Distribution Dynamics) rainfall-runoff model is the hydrological model used. The evaluation points out important information for the future seNorge2 developments: the daily mean temperature fields constitute an accurate and precise dataset, on average the predicted temperature has un unbiased estimate of the actual temperature and its precision (at grid points) varies between $0.8\,^{\circ}\mathrm{C}$ and $2.4\,^{\circ}\mathrm{C}$; the daily precipitation fields provide a reasonable estimate of the

Earth Syst. Sci. Data Discuss., https://doi.org/10.5194/essd-2017-64
Manuscript under review for journal Earth Syst. Sci. Data
Discussion started: 28 August 2017

Open Access Earth System Science Data Discussions

actual precipitation, the cross-validation shows that on average the precision of the estimates (at grid points) is about $\pm 20\%$, though a systematic underestimation of precipitation occurs in data-sparse areas and for intense precipitation. Both the seNorge snow and the DDD models have been able to make profitable use of seNorge2, partly because of the automatic calibration procedure they incorporate for precipitation. The dataset described in this article is available for public download at http://doi.org/10.5281/zenodo.845733.

1 Introduction

The successful modeling of hydrological processes requires reliable meteorological forcing data, which is a crucial but often undervalued element of the model chain (e.g., Magnusson et al., 2015). In Norway, the management of water and energy resources as well as forecasting of natural hazards relies largely on the results from hydrological modeling. The main operational hydrological models at the Norwegian Water Resources and Energy Directorate (NVE) use conventional (or observational) climatological daily gridded datasets of temperature and precipitation on a high-resolution grid as their input data.

Conventional climatological datasets are based on observed data only and they are used in several applications (Simmons et al., 2016). The Norwegian Meteorological Institute (MET) produces the *seNorge* collection of conventional gridded climate datasets, which are based on observations from climate and weather stations and archived in the Norwegian Climate Database. The seNorge data is used in the national forecasting system for floods, avalanches and landslides as well as for hydropower production planning. Consequently, the observation-based gridded dataset is of vital importance for both MET and NVE, and for several hydropower companies. They are also utilized for many other tasks, such as snow and permafrost mapping (Gisnås et al., 2017), research and climate-related analyses (Engen-Skaugen et al., 2007). Therefore, it is required to keep a high standard and quality of these data.

The seNorge version 1.0 was released in 1997 (Førland and Tveito, 1997) with focus on daily mean air temperature and accumulated precipitation for applications within fields such as climatology and hydrology. A detailed description of the method developed for the first seNorge release can be found in Tveito and Førland (1999); Tveito et al. (2000, 2002). Already the first applications required high-resolution meteorological fields in order properly represent the highly variable meteorological and topographical conditions of Norway, as well as a period covering several decades. Thus, the grid spacing was chosen to $1\,\mathrm{Km}$ in both meridional and zonal directions. The seNorge datasets covers the period from 1957 until today since it is continuously updated to serve daily operations both at NVE and MET.

In 2009, a seNorge version 1.1 (or simply *seNorge1.1*) was released and descriptions can be found in Mohr (2008, 2009). For this version, the spatial interpolation of temperature is based on a resid-

Earth Syst. Sci. Data Discuss., https://doi.org/10.5194/essd-2017-64
Manuscript under review for journal Earth Syst. Sci. Data
Discussion started: 28 August 2017

Open Access Earth System Science Data Discussions

ual kriging method, where the external trend parameterization is based on climatology. The daily precipitation is interpolated by a method based on triangulation, the input data is adjusted for the gauge undercatch due to wind and a systematic elevation dependence for precipitation is introduced. The seNorge1.1 dataset has been indirectly evaluated by applying snow models based on this data (Dyrrdal, 2010; Saloranta, 2012). In Saloranta (2012), a significant overestimation trend of the snow amounts with elevation was found by comparing model results with the observations of snow water equivalent (SWE) obtained from the hydropower companies. On the basis of this evaluation, a revised snow model (v.1.1.1) was introduced and a three-parameter elevation-dependent precipitation correction algorithm was optimized against the SWE observations (Saloranta, 2014b, a). The calibrated precipitation correction algorithm reduced the gridded input precipitation by up to 38% in the model simulations. The need for such a correction suggested that the vertical precipitation gradients (5-10% increase by $100\,$m elevation) as well as correction factors (up to $+80\%$) for precipitation measurement-gauge catch loss for solid precipitation could be too high. Moreover, the snow model data-assimilation study by Saloranta (2016) indicated too weak wintertime vertical temperature lapse rates in the seNorge1.1 dataset. Consequently, work was initiated to revise the spatial interpolation method and to establish an improved seNorge version 2.0 (or simply *seNorge2*) dataset for temperature and precipitation, which includes not only daily but also hourly aggregated variables.

seNorge2 is an ongoing project and it has a modular structure, which at its final stage would include: a) retrieval of temperature and precipitation observations from the Norwegian Climate Database; b) automatic data quality control; c) adjustment of solid precipitation for the wind undercatch; d) spatial interpolation based on statistical methods; e) post-processing of the predicted precipitation fields to adjust for bias; f) archiving and dissemination of temperature and precipitation gridded fields. In the current stage of development, not all the modules are activated. In particular, the solid precipitation is not adjusted for the wind undercatch and no post-processing (or calibration) of the final predictions is performed. In addition, the automatic data quality control setup is rather tolerant towards large deviations from the expected values. An advantage of the current seNorge2 setup is that a minimum number of parameters needs to be optimized. The scheme is robust, reasonably easy to test and makes use of all the available observations. The statistical interpolation scheme is based on Optimal Interpolation (OI: Gandin and Hardin, 1965) and it is flexible enough to incorporate additional information, such as geographical data.

In this study, we aim at evaluating the seNorge2 conventional datasets of daily temperature and precipitation, especially for snow- and hydrological modeling. In the future, we will increase the seNorge2 complexity and according to the outcomes of our evaluations we will prioritize our actions on the different modules. For the evaluation we rely on multi-year (around 60 years) gridded datasets to provide robust results. The quality assessment of the seNorge2 data is based on the summary statistics collected by leave-one-out cross-validation (CV) experiments. The indirect evaluation of seNorge2 has been carried out using NVEs operational snow- and hydrological models. In

Earth Syst. Sci. Data Discuss., https://doi.org/10.5194/essd-2017-64
Manuscript under review for journal Earth Syst. Sci. Data
Discussion started: 28 August 2017

Open Access Earth System Science Data Discussions

addition, we also assess the the consistency between the precipitation datasets and measured water balance components (catchment runoff and actual evapotranspiration). Finally, the results obtained with seNorge2 as forcing data have been compared with those obtained with seNorge1.1.

The outline of the paper is as follows. In section 2 the seNorge2 statistical interpolation methods are described, with the strongest emphasis on the procedures used for interpolating daily precipitation. Then, in section 3 seNorge2 is evaluated using both direct and indirect methods. Furthermore, in the same section the seNorge snow model and the DDD (Distance Distribution Dynamics) rainfall-runoff model are briefly presented.

2 Description of seNorge2

seNorge2 is a conventional climate dataset for daily temperature and precipitation that is updated daily and covers the period from 1957 onwards. The daily average temperature is defined as the arithmetic mean of 24 hourly values in the period 06-06 UTC. When hourly temperatures are not available, the daily mean temperature is calculated as a weighted mean of temperatures at 06, 12, 18 and 00 UTC (eventually the maximum and the minimum daily temperature) (Førland and Tveito, 1997). The daily total precipitation is defined as the accumulated precipitation in the time period 06-06 UTC.

The seNorge2 dataset is based on in situ observations from the Norwegian Climate Database. We also include data from the European Climate Assessment Dataset (ECA&D: Klein Tank et al., 2002) for regions neighboring Norway. Original non-homogenized time series have been used, to have a larger dataset than the one provided by the homogenized time series. The number of stations used for the interpolation varies with time due to data availability and the station distribution is uneven throughout the spatial domain. In Figure 1 the spatial distribution of all the stations in the region of interest for the period 1971-2010 is shown, together with the percentage of availability of their observations. On average, in the period 1980-2015 the number of observations used for the daily mean temperature is 480, while for the total precipitation is 920. However, the number of available observations is not stationary in time: for temperature there are more observations in recent years (the average in the period 2014-2015 is 660) while the situation is the opposite for precipitation (for the 80s around 1000 observations are available while the average is 820 for the period 2014-2015).

The statistical interpolation of temperature and precipitation are both based on modified OI schemes. OI has been developed as an objective analysis scheme for meteorological fields (Eliassen, 1954; Gandin and Hardin, 1965), then it has been widely used in data assimilation to provide initial conditions for numerical models (Kalnay, 2003; Daley, 1991; Lorenc, 1986). The use of a background or first-guess field is a central component of OI. The concept of first-guess field has been introduced in the context of objective analysis during the 1950s (Bergthörsson and Döös, 1955; Thompson, 1961) and it coincides with the prior information used in Bayesian statistical schemes. In our work, OI has

Earth Syst. Sci. Data Discuss., https://doi.org/10.5194/essd-2017-64
Manuscript under review for journal Earth Syst. Sci. Data
Discussion started: 28 August 2017

been used as a spatial interpolation technique and the background field has been estimated from the in situ observations instead of being an observation-independent information derived from numerical atmospheric models or climatology, as for the "classical" OI. For temperature, spatial interpolation schemes similar to the one implemented for seNorge2 can be found in Uboldi et al. (2008); Horel and Dong (2010) and in Frei (2014), though this last work is based on residual kriging instead of OI. For precipitation, Bayesian spatial interpolation schemes have been also applied in the past (Todini, 2001; Schiemann et al., 2010; Lussana et al., 2009; Aalto et al., 2016). However, the absence of an independent background motivated us to adopt an approach inspired by the successive-correction methods (Barnes, 1964) in the form proposed by Bratseth (1986). The spatial interpolation scheme developed for seNorge2 is based on an iteration of a statistical interpolation scheme over a decreasing sequence of spatial scales. This idea has been widely used for mesoscale meteorological analysis in successive-correction methods, see Uboldi and Buzzi (1994) and references therein. However, we have adapted this method to the special statistical properties of precipitation fields and its implementation can be regarded as an original contribution to this research field.

For both variables the spatial interpolation relies on the concept of scale-separation and the underlying idea is that the final predicted values are a combination of large scale and local scale effects. In our application, the term large scale refers to spatial scales that are significantly wider than the local station density, while the term local scale (or small scale) refers to spatial scales that are comparable to the local station density. The effects of atmospheric processes on scales that are smaller than the local station density are not properly resolved by the spatial interpolation schemes and they constitute the so-called representativeness error (Lussana et al., 2010), which is part of the observation error in OI. For example, small-scale processes are the result of very local responses to mesoscale dynamics that may affect just one or very few observations, thus determining large uncertainties in the final prediction. Because of the actual station distribution, it is expected that seNorge2 would properly resolve atmospheric processes from the synoptic down to the meso-β scale (Orlanski, 1975; Thunis and Bornstein, 1996), which has a lower bound of 20 Km.

The operational choices we have made were: (1) to use all available observations and (2) to keep the statistical interpolation settings fixed in time. As a result, any significant variation in time of the seNorge2 summary statistics should be attributed to an actual modification in the underlying climatology. However, as pointed out in Masson and Frei (2016), the variations in the station network impact on the estimation of long-term trends from conventional datasets. Further investigations are needed to accurately assess this impact on seNorge2.

In the following, the seNorge2 interpolation schemes are described in detail. Section 2.1 introduces briefly OI, highlighting the points which are useful for our purposes. Then, sections 2.2 and 2.3 describes the statistical interpolation schemes for temperature and precipitation, respectively. In particular, the spatial interpolation of precipitation is described in detail because of its originality.

Earth Syst. Sci. Data Discuss., https://doi.org/10.5194/essd-2017-64
Manuscript under review for journal Earth Syst. Sci. Data
Discussion started: 28 August 2017

Open Access Earth System Science Data Discussions

2.1 Optimal Interpolation

The OI aims at providing the best (i.e. minimum error variance for the analysis), linear, unbiased estimate of the unknown meteorological field by combining a prior information (i.e. background) on the grid with in situ observations. In the following, we use the same notation as Lussana et al. (2010) (based on Ide et al. (1997)): the vector $\mathbf{y}$ indicates the m observations of either air temperature or precipitation, and the vector $\mathbf{x}$ represents the n grid cells. Superscripts o, b and a denote observation, background and analysis, respectively; while the superscript t indicates the unknown true value. Matrices are in bold roman type (capital letters). Scalar variables are in italic type, so the i-th component of a vector $\mathbf{x}$ is x_i, while for a generic matrix $\mathbf{W}$, components are indicated as W_{ij}.

OI relies on the assumptions of Gaussian distribution for both the observation error $\boldsymbol{\varepsilon}^{\mathrm{o}} \equiv \mathbf{y}^{\mathrm{o}} - \mathbf{y}^{\mathrm{t}}$ and the background error $\boldsymbol{\varepsilon}^{\mathrm{b}} \equiv \mathbf{y}^{\mathrm{b}} - \mathbf{y}^{\mathrm{t}}$ (or $\boldsymbol{\eta}^{\mathrm{b}} \equiv \mathbf{x}^{\mathrm{b}} - \mathbf{x}^{\mathrm{t}}$ for grid points). As a consequence, their distributions are completely defined by their mean values and covariance matrices only. Both the observations and the background are assumed to be unbiased estimates of the true value and their error covariance matrices are specified by means of analytical functions, such that: $\boldsymbol{\varepsilon}^{\mathrm{o}} \sim N(\mathbf{0}, \mathbf{R})$, $\boldsymbol{\varepsilon}^{\mathrm{b}} \sim N(\mathbf{0}, \mathbf{S})$ and $\boldsymbol{\eta}^{\mathrm{b}} \sim N(\mathbf{0}, \mathbf{B})$. Furthermore, observations and background are regarded as uncorrelated variables.

The analysis is also a random variable with a Gaussian distribution (Jazwinski, 2007) and its mean values on the grid and at station locations can be written as:

$$\mathbf{x}^{\mathrm{a}} = \mathbf{x}^{\mathrm{b}} + \mathbf{K}\left(\mathbf{y}^{\mathrm{o}} - \mathbf{y}^{\mathrm{b}}\right) \quad (1)$$

$$\mathbf{y}^{\mathrm{a}} = \mathbf{y}^{\mathrm{b}} + \mathbf{W}\left(\mathbf{y}^{\mathrm{o}} - \mathbf{y}^{\mathrm{b}}\right) \quad (2)$$

where the two matrices of interpolation weights are: $\mathbf{K}$, the gain matrix; $\mathbf{W}$, the influence matrix.

The equations for the weight matrices $\mathbf{K}$ and $\mathbf{W}$ depend on our choices on the error covariance matrices. The observation error covariance matrix $\mathbf{R}$ is assumed to be diagonal and all the observations are assumed to have the same error variance σ_{o}^2, then: $\mathbf{R} \equiv \sigma_{\mathrm{o}}^2 \mathbf{I}$ ($\mathbf{I}$ is the identity matrix). The background error covariance matrices requires the specification of the correlation between two generic points $\mathbf{r}_i = (x_i, y_i, z_i)$ and $\mathbf{r}_j = (x_j, y_j, z_j)$, which for us is the correlation function ρ:

$$\rho(\mathbf{r}_i, \mathbf{r}_j) = \exp\left\{-\frac{1}{2}\left[\left(\frac{d(\mathbf{r}_i, \mathbf{r}_j)}{D^h}\right)^2 + \left(\frac{\Delta z(\mathbf{r}_i, \mathbf{r}_j)}{D^z}\right)^2\right]\right\} \quad (3)$$

Where: $d(\mathbf{r}_i, \mathbf{r}_j)$ is the horizontal distance between the two points ;$\Delta z(\mathbf{r}_i, \mathbf{r}_j)$ is the difference between their elevations; D^h and D^z are the horizontal and vertical de-correlation lengths, respectively. The generic component S_{ij} of the background error covariance matrix at station locations (a similar expression holds for $\mathbf{B}$ too) is $\mathrm{S}_{ij} \equiv \sigma_{\mathrm{b}}^2 \rho(\mathbf{r}_i, \mathbf{r}_j)$, where: $\mathbf{r}_i$ and $\mathbf{r}_j$ indicate the locations of the i-th and j-th stations, and the background error variance σ_{b}^2 is assumed to be the same for all the points. The components of the background error correlation matrix at station locations $\tilde{\mathbf{S}}$ can be written as $\tilde{\mathrm{S}}_{ij} \equiv \rho(\mathbf{r}_i, \mathbf{r}_j)$; while the background error correlation matrix between grid points and station loca-

Earth Syst. Sci. Data Discuss., https://doi.org/10.5194/essd-2017-64
Manuscript under review for journal Earth Syst. Sci. Data
Discussion started: 28 August 2017

tions is the $n \times m$ matrix with components $\tilde{\mathrm{G}}_{ij} \equiv \rho(\mathbf{r}_i, \mathbf{r}_j)$, where $\mathbf{r}_i$ indicates the spatial location of the i-th grid point and $\mathbf{r}_j$ is the j-th station location.

Given our assumptions on the error covariance matrices, the expressions for the weight matrices are derived directly from the theory of linear Kalman Filters (Uboldi et al., 2008):

$$\mathbf{K} = \tilde{\mathbf{G}} \left(\tilde{\mathbf{S}} + \varepsilon^2 \mathbf{I} \right)^{-1} \tag{4}$$

$$\mathbf{W} = \tilde{\mathbf{S}} \left(\tilde{\mathbf{S}} + \varepsilon^2 \mathbf{I} \right)^{-1} \tag{5}$$

where ε^2 is the ratio $\sigma_{\mathrm{o}}^2 / \sigma_{\mathrm{b}}^2$.

Two elements of the OI diagnostics are introduced in this paragraph, because they have been used in our work both for optimization of parameters and evaluation of results (sections 2.3-3). First, the Integrated Data Influence (IDI: Uboldi et al., 2008; Lussana et al., 2016) is the sensitivity of the analysis in a generic point on the domain to variations in the observations, independently from the actual observed values. In practice, the IDI field is the result of an OI scheme where the observations are set to 1 and the background is set to 0, such that regions where the observations effectively introduces information have IDI values close to 1. On the other hand, for data-void regions the IDI values are close to 0.

Second, the leave-one-out cross-validation (CV) analysis $\check{\mathbf{y}}^{\mathrm{a}}$: each component of the m-vector $\check{\mathbf{y}}^{\mathrm{a}}$ is the analysis value obtained for the corresponding station location by using all the other observations, but without using the observation measured at that station location. The equation for $\check{\mathbf{y}}^{\mathrm{a}}$ can be written as (Uboldi et al., 2008; Lussana et al., 2010):

$$\check{\mathbf{y}}^{\mathrm{a}} = \mathbf{y}^{\mathrm{o}} + \mathbf{w}^T \left(\mathbf{y}^{\mathrm{a}} - \mathbf{y}^{\mathrm{o}} \right) \tag{6}$$

where the vector $\mathbf{w}$ has components $w_i = (1 - W_{ii})^{-1}$. The deviation between the CV-analysis and its corresponding observation represents an estimate of the analysis error based on the idea that each observation is used as an independent verification of the analysis field. Because not all the available information is used, the error estimate can be regarded as a conservative one.

2.2 Spatial Interpolation of the daily mean temperature

The seNorge2 interpolation procedure used for temperature implements a two-steps scale-separation approach based on on a modification of the classical OI (section 2.1). A description of the method can be found in Lussana et al. (2017).

In the first step, a background field for the OI is estimated by means of spatial de-trending of the observed values. At each grid point, the background is meant to represent the temperature estimated not only from the few closest observations but also by considering a larger neighbourhood around the grid point. The size of this neighbourhood depends on the local station density and we refer to the background field as the large scale temperature field. The large scale field for the entire domain is obtained by blending several regional estimates of the large scale temperature, each of them

Earth Syst. Sci. Data Discuss., https://doi.org/10.5194/essd-2017-64
Manuscript under review for journal Earth Syst. Sci. Data
Discussion started: 28 August 2017

centered on a different geographical area. It is at the regional level that the spatial de-trending of observations is performed by using non-linear parametric functions of the geographical coordinates and elevation, which allow for temperature inversions in the thermal profile. Because the large scale field is computed at every time step, temporal variations of horizontal gradients or vertical profiles of temperature are automatically taken into account.

In the second step, the OI adjusts the background field locally, as in Eqs. (1)- (2), to add the effects of small scale processes (Uboldi et al., 2008). The procedure used to configure the OI is based on a trade-off between the necessity to adjust for the inclusion of small-scale processes for as many grid points as possible, and the need to keep a substantial distinction between large and local scale effects. The de-correlation length scales D^h and D^z, which are used in Eq. (3) to compute the background error covariance matrices, are set to: 60 Km and 600 m, respectively. As a general rule, D^h should be comparable to the average distance between one station and its closest three-four stations. The error variances are assumed constant over the spatial domain and we have set the observation error variance to half of the background error variance, such that $\varepsilon^2 = 0.5$.

To deal with the presence of gross measurement errors in the temperature observations, a spatial consistency test is included in the statistical interpolation, as described in Lussana et al. (2010).

2.3 Spatial Interpolation of the daily accumulated precipitation

The precipitation analysis is regarded as a composition of several (precipitation) events, which are considered individually, and the statistical properties of the field are allowed to change between events.

For each event, the statistical interpolation scheme has been implemented by means of an iterative algorithm on a *cascade* of spatial scales, from the synoptic scale down to the small-scale. As stated in Uboldi et al. (2008), given the filtering properties of OI, the choice of the scale parameters D^h and D^z in the correlation function ρ (Eq. (3)) determines a minimum distance scale (wavelength) resolved by the analysis. Besides, the spatial resolution observational network dictates a minimum for that choice and features so small that cannot be resolved by the observational network cannot be appropriately represented by the resulting analysis field. The iterative algorithm presented exploits the OI filtering properties. Starting from a first-guess of the average precipitation value (i.e. largest scale), several successive iterations of OI-derived corrections (over a decreasing sequence of values for D^h) are being applied to the predicted precipitation field.

In analogy with the scale-separation concept used for temperature in section 2.2, which is based on two scales, the idea adopted for precipitation might be regarded as a *multi*-scale separation approach.

The statistical interpolation scheme described in the following has been applied on Fennoscandia, with a focus on Norway. However, because of the online estimation of several parameters, it can be adapted and used for spatial interpolation in other geographical areas.

Earth Syst. Sci. Data Discuss., https://doi.org/10.5194/essd-2017-64
Manuscript under review for journal Earth Syst. Sci. Data
Discussion started: 28 August 2017

In the remaining of this section, the two main steps of the statistical interpolation scheme are described: the identification of individual precipitation events in section 2.3.1 and the multi-scale statistical interpolation scheme is section 2.3.2.

2.3.1 Identification of events

An individual event on the grid is a connected zone of grid points where the precipitation exceeds the predefined threshold of $0.1\,\mathrm{mm/day}$. Each event is considered as being independent from the others and the precipitation field is regarded as the union of several precipitation events spaced out between each other.

Initially, a first guess for the distribution of events both on the grid and for station locations is obtained. The observations measuring precipitation (i.e. *wet* observations) are tentatively grouped in events by using a triangulation-based procedure: two wet observations are assigned to the same event if a direct connection between them exists (i.e. they lie on the vertices of the same triangle) or if they are connected through only one observation not measuring precipitation (i.e. vertices of adjacent triangles). In this latter case, the observation not measuring precipitation (i.e. *dry* observation) is also included in the first guess of that event. Then, an interpolation procedure based on nearest neighbor is used to group grid points into events. The precipitation is set to $0\,\mathrm{mm}$ for all the grid points outside the event areas.

In the second step, each event is considered individually aiming at determining those grid points where precipitation is most likely to occur. The question is to decide whether the analysis at a grid point is more influenced by the surrounding wet observations or by the dry ones. As described in section 2.1, the influence on the analysis of a set of observations can be quantified through the IDI value. Suppose that the i-th grid point has been assigned in our first guess to a specific event, then precipitation is most likely to occur there if the IDI of the wet observations ($\mathbf{x}^{\mathrm{IDI}w}$) included in the event under consideration is greater or equal to a fraction of the IDI of the dry observations ($\mathbf{x}^{\mathrm{IDI}d}$):

$$x_i^{\mathrm{IDI}w} \geq 0.6 \cdot x_i^{\mathrm{IDI}d} \;\rightarrow\; \text{precipitation occurs at the } i\text{-th grid point} \tag{7}$$

We require that the influence of the dry observations $x_i^{\mathrm{IDI}d}$ must be considerably larger than $x_i^{\mathrm{IDI}w}$ for a grid point to be considered "dry". This can be regarded as a conservative choice, in case of uncertainty (i.e. when $x_i^{\mathrm{IDI}d}$ and $x_i^{\mathrm{IDI}w}$ are not too different) we prefer to estimate a precipitation value for the i-th grid point instead of taking the more drastic decision of setting it to zero. The factor 0.6 in Eq. (7) has been set as in (Lussana et al., 2009), because it improves the agreement between the model results and the observations. As described in section 2.1, the IDI values are obtained as the analysis values (Eq. (2)) with the background set to 0 and the observed values set to 1. In this case, the OI parameters used in the IDI elaboration can vary from grid point to grid point: D^h is the horizontal distance to the closest available station location (irrespective of the observed value); D^z is the maximum elevation within the event first-guess (a minimum value of $500\,\mathrm{m}$ is pre-set);

Earth Syst. Sci. Data Discuss., https://doi.org/10.5194/essd-2017-64
Manuscript under review for journal Earth Syst. Sci. Data
Discussion started: 28 August 2017

Open Access Earth System Science Data Discussions

$\varepsilon^2 \equiv \sigma_o^2/\sigma_b^2 = 0.1$, which means that we impose the IDI field to fit the value 1 in the surroundings of observation locations.

Finally, adjacent (connected) grid points where the precipitation is most likely to occur are assigned to the same event and the event gets a unique label. The wet observations are assigned to the same event of the surrounding grid points. In the special case of a wet observation surrounded by dry grid points only, a new event is created. The isolated wet observation is associated to this new event, together with the closest grid points. This special situation may occur in dense station areas (i.e. station density comparable to the grid resolution) when, for example, only one station is measuring precipitation.

2.3.2 Iterative Optimal Interpolation

As stated in section 2.3, the iterative algorithm operates on a cascade of spatial scales, which is defined through a decreasing sequence of K values for $D^h = \{\text{large scale}, \ldots, \text{local scale}\}$. The largest scale D_1^h is set to the semi-major axis of the ellipsoid of minimal area enclosing all grid points of the event under consideration (i.e. its ellipsoid hull), then $D_{k+1}^h = D_k^h - 10\text{Km}$ $(k = 1, \ldots, K)$ and the local scale D_K^h is set to the minimum distance between two stations (the minimum allowed value is $10\,\text{Km}$).

The regional topography influences the precipitation patterns, consequently points at the same elevation tend to be more correlated than points at different elevations. Because of that, we have decided to include elevation differences in our (de)correlation functions ρ (Eq. (3)). The sequence of K vertical scales D_k^z is not predefined, such as for D^h. On the contrary, they are optimized every time step and for each D_k^h value. The optimal D_k^z is chosen among four possible values $D^z = \{5000\text{m}, 2000\text{m}, 1000\text{m}, 500\text{m}\}$. A value of $D^z = 5000\text{m}$ means that the de-correlation of precipitation along the vertical is actually not needed, then the de-correlation gradually increases with decreasing D^z. By decreasing the correlation ρ between points, we are also reducing the spatial extent of the area of influence that every observation has on the analysis. Because our method is based only on observations, a predefined lower limit of 500m has been set for D^z, otherwise the total extension of data-sparse areas may become too large.

The application of the OI iterative scheme requires the definition of two further elements: 1) a spatial averaging operator $\langle \ldots \rangle_{h,v}$ to process the vector observed values. The operator is applied to its components to obtain for each station location a "processed observation" meant to represent the average precipitation in a neighbourhood of a predefined size around that location. The neighbourhood considered is a cylinder of radius h and height v, having its center of mass at the station location; 2) ε^2 (Eqs. (4)- (5)), the ratio between the observation and background error covariances ε^2 specifies the weight of the new information (i.e. the processed observations) compared to the background. At each iteration, the background is the result of previous iteration steps and it represents the integrated

Earth Syst. Sci. Data Discuss., https://doi.org/10.5194/essd-2017-64
Manuscript under review for journal Earth Syst. Sci. Data
Discussion started: 28 August 2017

Open Access Earth System Science Data Discussions

effect of the larger spatial scales. ε^2 is set to 0.1, as in the IDI calculation of section 2.3.1, and its value is kept constant in the elaboration.

The iterative OI algorithm is based on two nested loops.

- the *outer loop* over the $D^h = \{\text{large scale}, \ldots, \text{local scale}\}$ scales (index $k = 1, \ldots, K$). For the k-iteration, the background is the analysis obtained at iteration $k-1$: $\mathbf{x}^{\mathrm{b}}_k = \mathbf{x}^{\mathrm{a}}_{k-1}$ and $\mathbf{y}^{\mathrm{b}}_k = \mathbf{y}^{\mathrm{a}}_{k-1}$. As initial conditions, the vectors $\mathbf{x}^{\mathrm{b}}_1$ and $\mathbf{y}^{\mathrm{b}}_1$ are set to the mode of the distribution of observed precipitation values.

  - the *inner loop* over $D^z = \{5000\mathrm{m}, 2000\mathrm{m}, 1000\mathrm{m}, 500\mathrm{m}\}$ (index $c = 1, \ldots, 4$). The observation vector used is the processed observation $\mathbf{y}^{\mathrm{o}}_{k,c} \equiv \langle \mathbf{y}^{\mathrm{o}} \rangle_{D^h_k, D^z_c}$. First, the cross-validation analysis $\check{\mathbf{y}}^{\mathrm{a}}_{k,c}$ is computed as in Eq. (6), where the influence matrix $\mathbf{W}$ is computed using the pair $\left(D^h_k, D^z_c\right)$ in Eq. (3) to define the correlation function. Then, the optimal value for D^z ($\tilde{D}^z$) is chosen as the one that minimizes the relative error between $\check{\mathbf{y}}^{\mathrm{a}}_{k,c}$ and $\mathbf{y}^{\mathrm{o}}_{k,c}$ (i.e. relative error = prediction / observation). However, we are not using the actual (CV-) predicted and (processed) observed values in the definition of relative error. In fact, the "started logs" ($\mathrm{st.log}$) (Erdin, 2009; Rocke and Durbin, 2003) of those values have been used, so "to ensure an equal scaling of positive and negative deviations of prediction from observations and because the relative error is highly sensitive to small observations that might be under or overestimated by a large factor in the prediction" (Erdin, 2009). The relative error is written as:

$$rels_{k,c} = \sqrt{\frac{1}{m} \cdot \sum_{j=1}^{m} \left[\mathrm{st.log}\left(\check{y}^{\mathrm{a}}_{j,k,c}\right) - \mathrm{st.log}\left(y^{\mathrm{o}}_{j,k,c}\right) \right]^2} \tag{8}$$

  where $\ldots_{j,k,c}$ indicates the j-th vector component for iteration (k, c) and the started logs are defined as:

$$\mathrm{st.log}\,(x) = \begin{cases} \log_{10}(x) & \text{if } x > l_c, \\ \log_{10}(l_c) + (x - l_c) \,/\, [l_c \cdot \ln(10)] & \text{if } x \le l_c \end{cases} \tag{9}$$

  the critical threshold has been set to $l_c \equiv 1.5\,\mathrm{mm}$.

- out of the *inner loop* and back to the *outer loop*. the analyses $\mathbf{x}^{\mathrm{a}}_k$ (Eq. (1)) and $\mathbf{y}^{\mathrm{a}}_k$ (Eq. (2)) are obtained, the weight matrices $\mathbf{K}$ and $\mathbf{W}$ (Eqs. (4)- (5)) used in the analysis procedure are computed with the correlation function ρ (Eq. (3)) defined by the two parameters D^h and $\tilde{D}^z$.

The final analyses are $\mathbf{x}^{\mathrm{a}} = \mathbf{x}^{\mathrm{a}}_K$ and $\mathbf{y}^{\mathrm{a}} = \mathbf{y}^{\mathrm{a}}_K$.

3 Evaluation of seNorge2

The seNorge2 dataset has been evaluated by assessing both the quality of the gridded fields and the quality of the snow- and hydrological model results. The time period considered in our evaluation

Earth Syst. Sci. Data Discuss., https://doi.org/10.5194/essd-2017-64
Manuscript under review for journal Earth Syst. Sci. Data
Discussion started: 28 August 2017

ranges from 2000 to 2015, though each of the following sections consider a slightly different time interval within this period.

The seNorge2 daily products are directly evaluated by analyzing the summary statics collected through cross-validation. The object of this direct evaluation is to assess the quality of seNorge2 fields for general purposes, without addressing any particular application. In the case of daily averaged temperature, the evaluation is described in Lussana et al. (2016, 2017) where it has been shown that: on average the final analysis fields are an unbiased estimate of the actual two-meter temperature; the precision at grid points of our estimates varies between $0.8\,^{\circ}\mathrm{C}$ and $2.4\,^{\circ}\mathrm{C}$. For extremely low temperatures, e.g. below $-30\,^{\circ}\mathrm{C}$, a warm bias of around $1\,^{\circ}\mathrm{C}$ is present.

The evaluation of daily precipitation is presented in this paper. The direct evaluation of model output is reported in section 3.1. Besides, in section 3.2 the gridded precipitation dataset is also evaluated by assessing its consistency with the long-term water balance over a large number of Norwegian catchments. The last two sub-sections deal with the indirect evaluation of seNorge2. The dataset has been used as the input forcing for the seNorge snow model (section 3.3) and for the DDD hydrological model (section 3.4) and their results have been evaluated. The snow simulation results have been validated by using satellite observations of snow covered area, while the DDD hydrological model results have been compared with the measured stream flow.

3.1 Evaluation of daily precipitation fields

The time period considered in our evaluation covers 11 years, from 1 September 2003 to 31 August 2014. All the Norwegian stations shown in Figure 1 have been used in our evaluation.

Precipitation events characterized by length scales of comparable size with the local station density, which can reach several tenths of kilometers in sparse station areas (Figure 1), might be detected by just one station or not detected at all. In the case of isolated wet observations, the uncertainty in the predicted precipitation is expected to be quite large and it is not quantifiable through cross-validation. The statistics of occurrence for such cases is an indicator of the adequacy of the station network in detecting precipitation events and it may be interpreted as a lower limit for the atmospheric scales resolved by our network. The number of events observed by one station only is 44.520 (4% of all wet observations) and the median of their area distribution is $225\,\mathrm{Km}^2$, which correspond to a semi-major axis of the ellipsoid hull (section 2.3.2) equal to $13\,\mathrm{Km}$ (first quartile is $10\,\mathrm{Km}$, third quartile is $22\,\mathrm{Km}$). With reference to the hierarchy of atmospheric motions proposed by Thunis and Bornstein (1996), such length scales correspond to the lower boundary of the mesoscale (meso-γ) and they are consistent with the representation of: thunderstorms, thunderstorm groups and fronts.

In Figure 3, the distribution of relative error values for daily precipitation as a function of the precipitation intensity is shown. Note that the relative error we are using for evaluation is different from the one defined in section 2.3.2 for spatial interpolation purposes, though both make use of the cross-validation analysis (Eq. (6)). Consider the j-th station location, then the relative error is

Earth Syst. Sci. Data Discuss., https://doi.org/10.5194/essd-2017-64
Manuscript under review for journal Earth Syst. Sci. Data
Discussion started: 28 August 2017

defined as:

$$rel = \frac{\check{y}_j^{\mathrm{a}}}{y_j^{\mathrm{o}}} \tag{10}$$

Note that the relative error considered evaluates the analysis quality at grid points, even if both the CV-analysis and the observed values are quantities located at station points. In fact, by definition $\check{y}_j^{\mathrm{a}}$ is independent from y_j^{o} (this is not the case for y_j^{a}, of course), then $\check{y}_j^{\mathrm{a}}$ can be seen as the analysis at a grid point, which normally does not coincides with any of the station locations. The set of relative error values displayed in Figure 3 is obtained by considering all the station locations for every time step in the interval. The labels of the intensity classes reported on the abscissa in Figure 3 correspond to the following distribution quantiles: 25%, 50%, 75%, 95%, 99%.

The predicted values at grid points underestimate the actual precipitation, especially in the case of intense precipitation. The increase in magnitude of the deviation of the relative error from the ideal value of 1 with the increase of precipitation intensity is not surprising and it is related to the multiplicative error model which is in general valid for precipitation (Tian et al., 2013). For the most intense class of precipitation considered (i.e. observed values greater or equal to the 99% distribution quantile) the median of the distribution for the relative error is around 0.8, which corresponds to the distribution of CV-residuals (i.e. observation minus CV-analysis, not shown here) centered around $10\,\mathrm{mm}$ and with an interquartile range between $2\,\mathrm{mm}$ and $18\,\mathrm{mm}$. In general, the median of the different distributions is between .9 and 1 for the precipitation intensity classes up to $8\,\mathrm{mm}$ and the uncertainty (e.g. the interquartile range) is bounded between $\pm 20\%$ and $\pm 30\%$ of the observed value, which is a result comparable to the ones reported in previous studies (Isotta et al., 2014).

It is useful to consider the evaluation of each event separately to have an idea of the seNorge2 performances over regions and not only for a fixed set of points in space. For our event-based evaluation, we have extended the previous definition of relative error. Consider the event e, its relative error rel_x^e for observations greater or equal to x is:

$$rel_x^e = \mathrm{mean}\left(\check{y}_j^{\mathrm{a}}/y_j^{\mathrm{o}}\right) \text{ , } y_j^{\mathrm{o}} \text{ is assigned to event } e \text{ and } y_j^{\mathrm{o}} \geq x \tag{11}$$

The threshold x has been introduced to filter out the effect of weak precipitation, which might have a huge impact on the relative error (see the class "All" in Figure 3) but a minor effect on the overall water balance. The value of rel_x^e is then assigned to all the grid points within the ellipsoid hull associated with e.

In Figure 4, the mean value of $rel_{1\,\mathrm{mm}}^e$ over Norway is shown. The $rel_{1\,\mathrm{mm}}^e$ field shows a characteristics banding pattern, which is related to the typical trajectories followed by precipitation events in Norway: they frequently originate from low-pressure system over the Atlantic Ocean, moving their way eastward towards the Norwegian mainland. The distribution of $rel_{1\,\mathrm{mm}}^e$ is not uniform across the domain, the most significant underestimation of precipitation (i.e. $rel_{1\,\mathrm{mm}}^e$ between 0.9 and 0.95) occurs in the North and in a narrow strip of land in the South, while on average an overestimation of

Earth Syst. Sci. Data Discuss., https://doi.org/10.5194/essd-2017-64
Manuscript under review for journal Earth Syst. Sci. Data
Discussion started: 28 August 2017

Open Access Earth System Science Data Discussions

precipitation around 10% and 15% occurs in a region along the West coast in the South stretching towards the middle part of Norway. Our event-based evaluation has also shown that the deviation of the relative error from the ideal value of 1 increases with the event average intensity, as for the point based evaluation above.

3.2 Evaluating the precipitation grids using hydrological measurements

In this section, we evaluate the seNorge1.1 and seNorge2 precipitation datasets using stream flow measurements from 151 stations in Norway. These runoff measurements capture the outflow from catchments without artificial influence (e.g. hydropower) and glaciers. For the evaluation presented below we consider the period from 1 January 2000 to 31 December 2013. The map of the catchment sizes is shown in Figure 5, where each dot indicates the location of the catchment centroid and the colors display the size. Note that many of the smaller catchments are located in the wet and mountainous regions, thus showing higher runoff values than the larger catchments, which usually are located in flatter areas further inland with a comparably dry climate. For further details about the particular characteristics of the Norwegian catchments, see Vormoor et al. (2016).

Figure 6 shows the annual average catchment water balance as the losses of water (sum of runoff and actual evapotranspiration) against the inputs of water (precipitation). The actual evapotranspiration estimates were obtained from the MODIS Global Evapotranspiration Project (Mu et al., 2011). The regression lines are obtained through the application of a robust and resistant procedure as described in Lanzante (1996). seNorge1.1 shows higher annual total precipitation than the water losses for most catchments (coefficient of regression 1.08), while seNorge2 underestimates the input term in the water balance (coefficient of regression 0.63). The linear regressions between precipitation and the sum of runoff and evapotranspiration show an higher coefficient of determination (r^2) for seNorge1.1 than seNorge2. On the other hand, the seNorge2 points tend to lie closer to the regression line, as shown in the box on the upper left of Figure 6 where the regression residuals are reported for both versions. The sum of squares of residuals (i.e. residual = precipitation - predicted value by the linear regression) for seNorge1.1 is twice as large as the one for seNorge2: 12958521.8 $(\text{mm/year})^2$ for seNorge2 against 25435946.8 $(\text{mm/year})^2$ for seNorge1.1. As a consequence, seNorge2 provides less accurate but more precise estimates of the annual averaged precipitation than seNorge1.1.

Figures 7-8 show the ratio between accumulated precipitation and stream flow over the period from 1 January 2000 to 31 December 2013 for both seNorge versions. This ratio displays clear spatial patterns for both precipitation products (Figure 7). For seNorge1.1, the ratio is typically above 1.2 in the southern parts of Norway, and especially high in the south eastern part. Further north, the ratio varies within the range from 0.8 to 1.6. The ratio between precipitation and runoff is particularly high for catchments with an average runoff below approximately 1500 mm/year (Figure 8). For seNorge2, most catchments display a ratio between precipitation and runoff below 1.2 (Figure 7). Only in the south eastern corner of Norway, the interpolated precipitation values exceed the accumu-

Earth Syst. Sci. Data Discuss., https://doi.org/10.5194/essd-2017-64
Manuscript under review for journal Earth Syst. Sci. Data
Discussion started: 28 August 2017

lated runoff amounts. The ratio between precipitation and runoff decreases with increasing average yearly runoff (Figure 8). The spatial patterns in the ratio between precipitation and runoff indicate systematic errors for both precipitation products. For some regions, the large mismatch between the two variables cannot be attributed to the effect of evapotranspiration alone. The uncertainty in the runoff measurements should be taken into account and it could partly explain the very low or high ratios found in some areas. In particular, in the norther parts of Norway the uncertainty in the observed runoff is significant in the rivers during winter because of the ice formation.

Figures 9-10 shows the correlation coefficient between annual total precipitation and runoff for catchments on the Norwegian mainland. For computing the annual accumulation, we use the so-called hydrological year starting from the 1st of September. At this point in time during the year, most areas are snow-free and we assume that inter-annual variations in the total water storage in the catchments are small. For both precipitation products, the correlation coefficient shows rather high values in most parts of Norway (Figure 9). An exception is Finnmark, which is the northernmost region, where we have obtained lower values for the correlation coefficients than in most other regions. Finnmark is an area characterized by lower density of precipitation gauges than other parts of the country (Figure 1). Thus, the precipitation estimates from conventional datasets are affected by a higher degree of uncertainty for this region, if compared with the other areas of our spatial domain. For mid and southern parts of Norway, the seNorge1.1 precipitation displays slightly higher correlation coefficient than the seNorge2 product. This may indicate that the earlier version captures the inter-annual variations of precipitation better than the latest precipitation product. Figure 10 shows that the correlation coefficient is generally lower for catchments with average runoff below approximately 2000 mm/year than for watersheds with runoff above this threshold (Figure 10). Note that for catchments with low runoff, the relationship between precipitation and discharge is more influenced by evapotranspiration than for watersheds with high runoff.

3.3 Indirect evaluation through the seNorge snow model

Daily updated maps of snow conditions have been produced for Norway since 2004 by using the seNorge snow model (www.seNorge.no; Tveito et al., 2002; Engeset et al., 2004; Engeset et al.; Saloranta, 2012, 2014a, b, 2016) and the seNorge conventional climatological datasets as model forcing data. The simulated snow maps are used among others by the avalanche and flood forecasting services, hydropower energy situation analysis, as well as the general public. The seNorge snow model consists of two main submodels, namely 1) the SWE submodel for snow pack water balance and 2) the snow compaction and density submodel for converting SWE to snow depth. The equations and default parameters of the seNorge snow model (v.1.1.1) are presented in Saloranta (2016).

Briefly described, the SWE submodel (v.1.1.1) uses a threshold air temperature to separate between snow and rain precipitation, handles separately the ice and liquid water fractions of the total SWE and keeps track of the accumulation and melting of snow. The snowpack can retain liquid water

Earth Syst. Sci. Data Discuss., https://doi.org/10.5194/essd-2017-64
Manuscript under review for journal Earth Syst. Sci. Data
Discussion started: 28 August 2017

from snow melt and rain up to a fraction of its ice content, while the excess goes to runoff. The liquid water in snow pack can also be refrozen to ice. The daily snow melt rate is a function of air temperature and solar radiation. The two melt model parameters are estimated using the extensive melt rate data from Norwegian snow pillows (Saloranta, 2014a). Moreover, the average grid cell snow melt rates are also affected by the simulated fraction of snow-covered area (SCA) in the model grid cells. The SCA algorithm assumes that snow is distributed as the uniform distribution $U(\min, \max)$ within the grid cells, i.e. that all SWE values between a defined minimum and maximum value are equally likely within the snow-covered part of the grid cell (Saloranta, 2014a, 2016).

In the evaluation, the seNorge snow model is run with the temperature and precipitation from the seNorge1.1 and seNorge2 conventional climatological datasets as forcing in the period 2001-2015, and the simulated SCA values in each of the approximately 320000 simulated grid cells are compared to the corresponding observed SCA values based on MODIS (moderate resolution imaging spectroradiometer; http://modis.gsfc.nasa.gov/) satellite images. No specific model calibration has been done prior to this evaluation.

The set of MODIS satellite images, selected on the basis of manual pre-viewing for this study, consist of 1123 images in the period 2001-2015. For each MODIS satellite scene, each pixel (500 x 500 meters) is assigned a SCA value between 0-100% coverage using a method based on the Norwegian linear reflectance to snow cover algorithm (NLR) (Solberg et al., 2006). The input to the NLR algorithm is the normalized difference snow index signal (NDSI- signal) (Salomonson and Appel, 2004). An area-weighted mean of the nine MODIS grid cells overlapping with a 1 x 1 Km seNorge grid cell is calculated to produce a SCA-value for comparison with the snow model. Moreover, those MODIS grid cells, where 1) the slope is steeper than 22 degrees (corresponding to a 200 m elevation change per 500 m horizontal distance), or where 2) the elevation difference between MODIS and seNorge grid cells is exceeding $\pm$100m, or where 3) at least one of the eight surrounding MODIS grid cells is located on seawater, are not used in calculating the weighted mean. The MODIS grid cells may also be classified as cloud-covered and thus give no information on SCA. If the included MODIS grid cells with SCA values cover less than 25% of the seNorge grid area, no weighted mean SCA value is calculated for the particular seNorge grid cell. This occurs in 7% of the seNorge grid cells due to the three topographical constraints alone, as listed above.

In the evaluation, for each day when a satellite image is available, each seNorge grid cell is classified into three categories: model under- or overestimation, or good match. A good match is here defined as when the difference in the simulated and observed SCA is not exceeding $\pm$ 50%-points. These three categories are also assigned a score of -1, 0 and $+1$, respectively. This type of classification is applied in order to make the analysis more robust to systematic errors that can be present in the observed satellite-based SCA e.g., due to the effect of forest canopy over the snow-covered area.

In order to make regional summaries of the evaluation results, Norway is divided into eastern, western and northern regions and the fraction of the region's grid cells where the model simulations

Earth Syst. Sci. Data Discuss., https://doi.org/10.5194/essd-2017-64
Manuscript under review for journal Earth Syst. Sci. Data
Discussion started: 28 August 2017

Open Access Earth System Science Data Discussions

Table 1. 90% percentile values of the model under- (F_u) and overestimation (F_o) (in % of grid cells) in the three regions and for the two version of the conventional climate dataset.

90% percentile F_u, F_o	Eastern	Western	Northern
seNorge1.1	7%, 13%	7%, 12%	5%, 6%
seNorge2	8%, 4%	7%, 5%	18%, 3%
seNorge2(*)	8%, 5%	7%, 5%	18%, 2%

(*) based only on data from the Norwegian climate database, without using ECA&D data outside Norway.

significantly under- (F_u) and overestimate (F_o) in comparison to the observed SCA (i.e., a deviation exceeding ± 0.5), are calculated for each day a satellite image is available.

As the maximum deviation between observed and simulated SCA may occur at different times in different elevations and regions, a monthly mean of the model fit category scores (-1, 0,$+1$) is calculated for each seNorge grid cell and month (if at least 15 score-values are available for the particular grid cell and month). Then, a bias index B is defined for each grid cell by summing up the minimum and the maximum values (i.e. the largest under- and overestimations) of the monthly mean scores (if at least three monthly means are available). This index B should reflect the systematic bias (if any) in simulated SCA in the particular grid cell encountered during the period from March to July.

The regional model under- and overestimation (F_u , F_o) of the SCA, based on totally 369, 318 and 265 images in eastern, western and northern Norway, respectively, are shown in Figure 11. The 90% percentile values of F_u and F_o are shown in Table 1. These results show that the snow model run with seNorge1.1 data forcing clearly overestimates the SCA in the main melting season (May-June) in eastern and western Norway (Figure 11). When the snow model is run with the seNorge2 data forcing, the average F_u and F_o are roughly within a 5% deviation level for the whole analysis period from March to July in eastern and western Norway (Figure 11). For seNorge2, no significant overestimation is detected, but there is a slight tendency to more under- than overestimation, which can be attributed to the use of precipitation observations, which have not yet been adjusted for the gauge-catch error. In the northern Norway, however, the results show a different pattern, where the snow model run with seNorge1.1 data forcing performs rather well, while the model application based on seNorge2 data forcing significantly underestimates the SCA in May-June (Figure 11; Table 1).

The maps of the bias index B (Figure 12) reveal the patterns of SCA overestimation in eastern and western Norway when using seNorge1.1 data, and of SCA underestimation in northern Norway when using seNorge2 data. The index B shows a positive correlation with elevation when using the seNorge1.1 dataset (correlation coefficient of 0.56, 0.37 and 0.19 for eastern, western and northern regions, respectively), while for the seNorge2 dataset correlation of B with elevation is near zero for the eastern and western regions, and negative (-0.25) for the northern region.

Earth Syst. Sci. Data Discuss., https://doi.org/10.5194/essd-2017-64
Manuscript under review for journal Earth Syst. Sci. Data
Discussion started: 28 August 2017

3.4 Indirect evaluation through the DDD model

The rainfall-runoff model DDD (Distance Distribution Dynamics) (Skaugen and Onof, 2014; Skaugen and Mengistu, 2016) has been calibrated using the seNorge2 meteorological grid for 136 Norwegian catchments located all over Norway (see Figure 14 for the geographical distribution of catchments). Input to the DDD model is only precipitation and temperature and the model is semi-distributed in that the moisture-accounting (rainfall and snow melt) is performed for 10 elevation zones of equal area. DDD has a 2-dimensional representation of the subsurface reservoir allowing for spatial variability of groundwater levels as a function of distance from the river-network. Similar to the seNorge snow model, snow melt is estimated using a calibrated temperature index model (without the additional radiation term) and a calibrated threshold temperature separating solid and liquid precipitation. The runoff dynamics of the DDD are characterized by a parsimonious parameter regime where the parameters are individually estimated from Geographical Information Systems (GIS) or from observed runoff records (recession analysis) and not collectively against observed runoff. Estimating the parameters in such a way reduces the tendency of model parameters when calibrated as a set, to collectively compensate for errors in input data and model structure, and hence acquire unrealistic values. DDD is calibrated optimizing the Kling-Gupta Efficiency (KGE) skill-score (Kling et al., 2012) where the parameters are optimized so that correlation is maximized, variability is reproduced and bias is minimized.

The model parameters for the 136 catchments have been calibrated for the period 1 September 2000 to 31 December 2014 and validated for the period 1 September 1985 to 31 August 2000.

The mean KGE for the 136 catchments is 0.87, and the mean bias is 0.1%, indicating that the volume of observed and simulate runoff was practically the same. Crucial for obtaining such a low bias was the ability in DDD to adjust the amount of precipitation obtained from the meteorological grids. The adjustment is made through a correction factor that linearly increases/decreases the precipitation in the course of the calibration. DDD has the ability to use different correction factors for precipitation as liquid (rain P_{corr}) or solid (snow S_{corr}).

The correction factor S_{corr} should be higher than P_{corr} due to the expected greater under-catch for snow compared to liquid precipitation. However, for a calibrated parameter set, this is not always the case. For this study, the calibrated correction factors for precipitation and snow are meant to evaluate the seNorge2 dataset.

Figure 13 shows the statistics of simulated precipitation P (precipitation multiplied by the correction factor), actual evapotranspiration (AE) and the ratio between simulated AE and P. In general, the water balance seems reasonable, although the simulated AE shows lower values if compared with the ones reported in section 3.2 and it displays a rather high variability. Values of AE lower than the expected ones indicate that the correction factors are also too low, since the runoff volumes have reasonable values. So, with the understanding of a possible underestimation of AE, we inter-

Earth Syst. Sci. Data Discuss., https://doi.org/10.5194/essd-2017-64
Manuscript under review for journal Earth Syst. Sci. Data
Discussion started: 28 August 2017

pret the calibrated corrections as indicators of under/overestimation of precipitation in the seNorge2 meteorological grid.

Figures 14-15 show the calibrated P_{corr} and S_{corr} values plotted according to the centroid of the catchment they represent. Furthermore, in the two Figures the histograms of the calibrated P_{corr} and S_{corr} values are plotted. We see that the mean value for P_{corr} is well beyond 1.0. The geographical distribution of P_{corr} reveals that seNorge2 underestimates liquid precipitation on the west coast along the country and in the mountains. For solid precipitation Figure 15 shows that S_{corr} is more evenly distributed around the mean value which is close to 1.0. The geographical distribution of S_{corr} is quite similar to that of P_{corr} although the underestimation of precipitation as snow is quite pronounced in the northern Norway.

3.5 Discussion on the evaluation of daily precipitation

The direct evaluation of the seNorge2 products shows that: the station network is, on average, too sparse to detect all small scale precipitation events, such as isolated thunderstorms, occurring within our domain; from cross-validation, the bias of the analysis at grid points is significant only for intense precipitation, which is underestimated, and the uncertainty is bounded between $\pm 20\%$, or $\pm 30\%$, of the analysis value; by considering average statistics on precipitation events, and not on individual observations, the average of the relative error varies between 0.9 and 1.15 over Norway, with the lower values in northern Norway and in a small area in the south of the domain.

The comparison of seNorge2 with the measurements of the long-term water balance shows that: seNorge2 tends to underestimate precipitation and, if compared to the previous seNorge version based on triangulation, it provides less accurate but more precise estimates of the annual averaged precipitation, moreover the inter-annual variations of precipitation in some areas with a data-sparse network are better represented in the previous version.

The indirect evaluations of seNorge2 by considering the performances of the seNorge snow model and of the DD model show that: for snow, a significant underestimation has been detected in northern Norway, while for the rest of the country the estimates are in reasonable agreement with the observations; for liquid precipitation, underestimation occurs along the west coast of Norway and in the mountains. seNorge2, as a whole dataset, is an improvement of seNorge1.1 for e.g. snow mapping application in southern Norway, where the model can take advantage of both the improved temperature and precipitation datasets, as shown in section 3.3. The seNorge snow model is likely to be more sensitive to air temperature then the DDD rainfall-runoff model, thus taking advantage of both the improved precipitation and temperature fields in seNorge2 for southern Norway. It is worth noting that in the indirect model evaluations, the deviations between the simulated and observed SCA or discharge can also arise due to the model parameter uncertainty as well as due to the uncertainty in how well the model code, algorithms, and the applied daily time step represent the real hydrological processes in nature.

Earth Syst. Sci. Data Discuss., https://doi.org/10.5194/essd-2017-64
Manuscript under review for journal Earth Syst. Sci. Data
Discussion started: 28 August 2017

As stated in the Introduction, seNorge2 is a modular project and some of its modules still need to be implemented. In the following, from the lessons learned from evaluation, possible future developments are discussed. There are three main points that must be considered. First, we have decided to use the measured precipitation data without any adjustment for wind-induced gauge undercatch. In principle, such an adjustment would introduce an additional source of uncertainty in the representation of the spatial structure of the precipitation fields by means of point measurements. However, as shown by the indirect evaluation, the amount of actual precipitation which is not observed by the gauges can become a significant portion of the total precipitation and it might impact on the spatial structure of the field, especially for solid precipitation (Førland and Tveito, 1997; Wolff et al., 2015). Second, the impact of station density on the quality of the precipitation fields (e.g. intensity and intermittency) should be better investigated. For statistical interpolation methods, the density of the station network is the main control on spatial patterns of the interpolation skill (Hofstra et al., 2008). Besides, variations in the station density impact differently on the percentiles of the distribution of analyzed values and, on average, higher percentiles are smoothed out by sparse station networks (Hofstra et al., 2010). Eventually, a post-processing procedure could be used for those areas characterized by a rather sparse network of observations. As for the third point, a statistical model of the relationship between precipitation and topography should be introduced in our interpolation scheme. In Masson and Frei (2014), the use of interpolation methods with multi-scale topographic predictors has been investigated and their results show that a statistical method (kriging with external drift in their case, which is similar to OI) with a realistic description of the spatial covariance function (i.e. the $\mathbf{S}$ and $\mathbf{B}$ matrices defined in section 2.1, then ultimately the ρ function in Eq. (3)) and the use of a single topographic predictor yield accurate precipitation gridded datasets. In particular, a climatological field, which incorporates the effect of topography on precipitation, used as the background in the statistical interpolation of daily precipitation provided the better results in complex terrain.

4 Conclusions

The seNorge version 2.0 (seNorge2) gridded dataset for daily mean temperature and daily total precipitation on Norway is described in this paper. The dataset is based on in situ observations only and it is continuously updated, at least once a day, while the archive goes back in time to 1957. The main objective of the dataset is to support climate and hydrology applications and it is presented on a high-resolution grid having 1 Km of grid spacing in both zonal and meridional directions.

The spatial interpolation schemes for both temperature and precipitation rely on statistical (Bayesian) methods, where the final predicted field is regarded as being determined by the integrated effects of atmospheric motions at different spatial scales. For daily mean temperature, the scale-separation approach developed combines a background field representing a larger-scale temperature field with the information on small-scale processes as observed locally by the in situ observations. The spa-

Earth Syst. Sci. Data Discuss., https://doi.org/10.5194/essd-2017-64
Manuscript under review for journal Earth Syst. Sci. Data
Discussion started: 28 August 2017

tial interpolation of daily total precipitation is based on a combination of two classical interpolation schemes, namely Optimal Interpolation and successive-correction methods. An original multi-scale-separation approach has been implemented by means of a statistical interpolation scheme where the information is passed through a cascade of (decreasing) spatial scales, which potentially could cover scales from the synoptic motions down to the lower boundary of the mesoscale.

The evaluation of seNorge2 is based on systematic leave-one-out cross-validations. The temperature fields are unbiased estimates of the actual temperature for most part of the temperature range, only for extremely low temperatures a warm bias of around $1\,^{\circ}\mathrm{C}$ is present. The precision of the temperature field varies between $0.8\,^{\circ}\mathrm{C}$ and $2.4\,^{\circ}\mathrm{C}$ for daily average temperature. The quality of the precipitation fields varies across the domain and with the precipitation intensity. Intense precipitation is more likely to be underestimated than weak precipitation. On average, the uncertainty of the predicted precipitation values at a grid point is approximately $\pm 20\%$ or $\pm 30\%$, depending on precipitation intensity.

In this article, we have focused on the evaluation of precipitation and the gridded fields have been compared with hydrological measurements to assess their consistency with the observed water balance. The previous seNorge version has also been used as a reference in the evaluation. By evaluating the output of snow and hydrological models that make use of seNorge2 as meteorological input, the quality of the seNorge2 products (both temperature and precipitation) has also been evaluated indirectly. Both models provide realistic outcomes and seNorge2 constitutes a valuable resource for hydrology. At the same time, our evaluation points out that seNorge2 underestimates precipitation, especially liquid precipitation and in data-sparse areas, such as northern Norway and the mountainous region in Southern Norway.

The seNorge project at MET Norway has the objective of maintaining and improving the conventional climate datasets of daily temperature and precipitation. The seNorge2 dataset (release 17.08) is publically available via http://doi.org/10.5281/zenodo.845733. Users can also access fresher, more recent data for daily temperature at http://thredds.met.no/thredds/catalog/metusers/senorge2/seNorge2/provisional_archive/TEMP1d/gridded_dataset/catalog.html and for precipitation at http://thredds.met.no/thredds/catalog/metusers/senorge2/seNorge2/provisional_archive/TEMP1d/gridded_dataset/catalog.html. Furthermore, the data are shown on the web-portals senorge.no and xgeo.no (both in Norwegian only).

Acknowledgements. Work at MET Norway and NVE on the activities presented in the article has been funded by the Norwegian project ”Felles aktiviteter NVE-MET tilknyttet nasjonal flom- og skredvarslingstjeneste” and NVE-project ”FoU-80200”.

Earth Syst. Sci. Data Discuss., https://doi.org/10.5194/essd-2017-64
Manuscript under review for journal Earth Syst. Sci. Data
Discussion started: 28 August 2017

Open Access Earth System Science Data Discussions

References

Aalto, J., Pirinen, P., and Jylhä, K.: New gridded daily climatology of Finland: Permutation-based uncertainty estimates and temporal trends in climate, Journal of Geophysical Research: Atmospheres, 121, 3807–3823, 2016.

Barnes, S. L.: A technique for maximizing details in numerical map analysis, J. Appl. Meteorol., 3, 395–409, 1964.

Bergthörsson, P. and Döös, B. R.: Numerical weather map analysis, Tellus, 7, 329–340, 1955.

Bratseth, A.: Statistical Interpolation by means of successive corrections, Tellus, 38A, 439–447, 1986.

Daley, R.: Atmospheric Data Analysis, Cambridge University Press, 1991.

Dyrrdal, A. V.: An evaluation of Norwegian snow maps: simulation results versus observations, Hydrology Research, 41, 27–37, 2010.

Eliassen, A.: Provisional report on calculation of spatial covariance and autocorrelation of the pressure field, Inst. Weather and Clim. Res., Acad. Sci., Oslo, Tech. Rep, 5, 1954.

Engen-Skaugen, T., Haugen, J. E., and Tveito, O. E.: Temperature scenarios for Norway: from regional to local scale, Climate Dynamics, 29, 441–453, 2007.

Engeset, R., Tveito, O. E., Udnæs, H.-C., Alfnes, E., Mengistu, Z., Isaksen, K., and Førland, E. J.: Snow map validation for Norway.

Engeset, R., Tveito, O. E., Udnæs, H.-C., Alfnes, E., Mengistu, Z., Isaksen, K., and Førland, E. J.: Snow map validation for Norway, in: Proceedings XXIII Nordic Hydrological Conference 2004, pp. 8–12, 2004.

Erdin, R.: Combining rain gauge and radar measurements of a heavy precipitation event over Switzerland: Comparison of geostatistical methods and investigation of important influencing factors, Ph.D. thesis, Bundesamt für Meteorologie und Klimatologie, MeteoSchweiz, 2009.

Førland, E. and Tveito, O.: Temperatur og snødata for flomberegning, DNMI Report, 28, 51, 1997.

Frei, C.: Interpolation of temperature in a mountainous region using nonlinear profiles and non-Euclidean distances, International Journal of Climatology, 34, 1585–1605, 2014.

Gandin, L. S. and Hardin, R.: Objective analysis of meteorological fields, vol. 242, Israel program for scientific translations Jerusalem, 1965.

Gisnås, K., Etzelmüller, B., Lussana, C., Hjort, J., Sannel, A. B. K., Isaksen, K., Westermann, S., Kuhry, P., Christiansen, H. H., Frampton, A., et al.: Permafrost Map for Norway, Sweden and Finland, Permafrost and Periglacial Processes, 28, 359–378, 2017.

Hofstra, N., Haylock, M., New, M., Jones, P., and Frei, C.: Comparison of six methods for the interpolation of daily, European climate data, Journal of Geophysical Research: Atmospheres, 113, 2008.

Hofstra, N., New, M., and McSweeney, C.: The influence of interpolation and station network density on the distributions and trends of climate variables in gridded daily data, Climate dynamics, 35, 841–858, 2010.

Horel, J. D. and Dong, X.: An evaluation of the distribution of Remote Automated Weather Stations (RAWS), Journal of Applied Meteorology and Climatology, 49, 1563–1578, 2010.

Ide, K., Courtier, P., Ghil, M., and Lorenc, A.: Unified notation for data assimilation: operational, sequential and variational, Practice, 75, 181–189, 1997.

Isotta, F. A., Frei, C., Weilguni, V., Perčec Tadić, M., Lassegues, P., Rudolf, B., Pavan, V., Cacciamani, C., Antolini, G., Ratto, S. M., et al.: The climate of daily precipitation in the Alps: development and analysis

of a high-resolution grid dataset from pan-Alpine rain-gauge data, International Journal of Climatology, 34, 1657–1675, 2014.

Jazwinski, A. H.: Stochastic processes and filtering theory, Courier Dover Publications, 2007.

Kalnay, E.: Atmospheric Modeling, Data Assimilation and Predictability, Cambridge University Press, 2003.

Klein Tank, A., Wijngaard, J., Können, G., Böhm, R., Demarée, G., Gocheva, A., Mileta, M., Pashiardis, S., Hejkrlik, L., Kern-Hansen, C., et al.: Daily dataset of 20th-century surface air temperature and precipitation series for the European Climate Assessment, International journal of climatology, 22, 1441–1453, 2002.

Kling, H., Fuchs, M., and Paulin, M.: Runoff conditions in the upper Danube basin under an ensemble of climate change scenarios, Journal of Hydrology, 424, 264–277, 2012.

Lanzante, J. R.: Resistant, robust and non-parametric techniques for the analysis of climate data: theory and examples, including applications to historical radiosonde station data, International Journal of Climatology, 16, 1197–1226, 1996.

Lorenc, A.: Analysis methods for numerical weather prediction, Quart. J. Roy. Meteorol. Soc., 112, 1177–1194, 1986.

Lussana, C., Salvati, M., Pellegrini, U., and Uboldi, F.: Efficient high-resolution 3-D interpolation of meteorological variables for operational use, Advances in Science and Research, 3, 105–112, 2009.

Lussana, C., Uboldi, F., and Salvati, M. R.: A spatial consistency test for surface observations from mesoscale meteorological networks, Quarterly Journal of the Royal Meteorological Society, 136, 1075–1088, 2010.

Lussana, C., Tveito, O. E., and Uboldi, F.: seNorge v2.0: an observational gridded dataset of temperature for Norway, 2016.

Lussana, C., Tveito, O. E., and Uboldi, F.: Three-dimensional spatial interpolation of two-meter temperature on Norway, submitted to the Quarterly Journal of the Royal Meteorological Society, 2017.

Magnusson, J., Wever, N., Essery, R., Helbig, N., Winstral, A., and Jonas, T.: Evaluating snow models with varying process representations for hydrological applications, Water Resources Research, 51, 2707–2723, 2015.

Masson, D. and Frei, C.: Spatial analysis of precipitation in a high-mountain region: exploring methods with multi-scale topographic predictors and circulation types, Hydrology and Earth System Sciences, 18, 4543, 2014.

Masson, D. and Frei, C.: Long-term variations and trends of mesoscale precipitation in the Alps: recalculation and update for 1901–2008, International Journal of Climatology, 36, 492–500, 2016.

Mohr, M.: New routines for gridding of temperature and precipitation observations for “seNorge. no”, Met. no Report, 8, 2008, 2008.

Mohr, M.: Comparison of versions 1.1 and 1.0 of gridded temperature and precipitation data for Norway, Norwegian Meteorological Institute, met no note, 19, 2009.

Mu, Q., Zhao, M., and Running, S. W.: Improvements to a MODIS global terrestrial evapotranspiration algorithm, Remote Sensing of Environment, 115, 1781–1800, 2011.

Orlanski, I.: A rational subdivision of scales for atmospheric processes, Bulletin of the American Meteorological Society, 56, 527–530, 1975.

Rocke, D. M. and Durbin, B.: Approximate variance-stabilizing transformations for gene-expression microarray data, Bioinformatics, 19, 966–972, 2003.

Earth Syst. Sci. Data Discuss., https://doi.org/10.5194/essd-2017-64
Manuscript under review for journal Earth Syst. Sci. Data
Discussion started: 28 August 2017

Salomonson, V. and Appel, I.: Estimating fractional snow cover from MODIS using the normalized difference snow index, Remote sensing of environment, 89, 351–360, 2004.

Saloranta, T.: Simulating snow maps for Norway: description and statistical evaluation of the seNorge snow model, The Cryosphere, 6, 1323–1337, 2012.

Saloranta, T.: New version (v. 1.1. 1) of the seNorge snow model and snow maps for Norway, Rapport 6-2014, 2014a.

Saloranta, T.: Simulating more accurate snow maps for Norway with MCMC parameter estimation method, The Cryosphere Discussions, 8, 1973–2003, 2014b.

Saloranta, T. M.: Operational snow mapping with simplified data assimilation using the seNorge snow model, Journal of Hydrology, 538, 314–325, 2016.

Schiemann, R., Liniger, M. A., and Frei, C.: Reduced space optimal interpolation of daily rain gauge precipitation in Switzerland, Journal of Geophysical Research: Atmospheres, 115, n/a–n/a, doi:10.1029/2009JD013047, http://dx.doi.org/10.1029/2009JD013047, 2010.

Simmons, A., Berrisford, P., Dee, D., Hersbach, H., Hirahara, S., and Thépaut, J.-N.: A reassessment of temperature variations and trends from global reanalyses and monthly surface climatological datasets, Quarterly Journal of the Royal Meteorological Society, 2016.

Skaugen, T. and Mengistu, Z.: Estimating catchment-scale groundwater dynamics from recession analysis-enhanced constraining of hydrological models, Hydrology and Earth System Sciences, 20, 4963, 2016.

Skaugen, T. and Onof, C.: A rainfall-runoff model parameterized from GIS and runoff data, Hydrological Processes, 28, 4529–4542, 2014.

Solberg, R., Amlien, J., and Koren, H.: A review of optical snow cover algorithms. Norwegian Computing Center Note, no, Tech. rep., SAMBA/40/06, 2006.

Thompson, P. D.: Numerical weather analysis and prediction, Macmillan, 1961.

Thunis, P. and Bornstein, R.: Hierarchy of mesoscale flow assumptions and equations, Journal of the atmospheric sciences, 53, 380–397, 1996.

Tian, Y., Huffman, G. J., Adler, R. F., Tang, L., Sapiano, M., Maggioni, V., and Wu, H.: Modeling errors in daily precipitation measurements: Additive or multiplicative?, Geophysical Research Letters, 40, 2060–2065, 2013.

Todini, E.: A Bayesian technique for conditioning radar precipitation estimates to rain-gauge measurements, Hydrology and Earth System Sciences Discussions, 5, 187–199, 2001.

Tveito, O., Førland, E., Heino, R., Hanssen-Bauer, I., Alexandersson, H., Dahlström, B., Drebs, A., Kern-Hansen, C., Jónsson, T., Vaarby Laursen, E., et al.: Nordic temperature maps, DNMI report, 9, 2000.

Tveito, O. E. and Førland, E. J.: Mapping temperatures in Norway applying terrain information, geostatistics and GIS, Norsk Geografisk Tidsskrift-Norwegian Journal of Geography, 53, 202–212, 1999.

Tveito, O. E., Udnæs, H.-C., Mengistu, Z., Engeset, R., and Førland, E. J.: New snow maps for Norway, in: Proceedings XXII Nordic Hydrological Conference 2002, pp. 527–532, 2002.

Uboldi, F. and Buzzi, A.: Successive-correction methods applied to mesoscale meteorological analysis, Il Nuovo Cimento C, 17, 745–761, 1994.

Uboldi, F., Lussana, C., and Salvati, M.: Three-dimensional spatial interpolation of surface meteorological observations from high-resolution local networks, Meteorological Applications, 15, 331–345, 2008.

Earth Syst. Sci. Data Discuss., https://doi.org/10.5194/essd-2017-64
Manuscript under review for journal Earth Syst. Sci. Data
Discussion started: 28 August 2017

Vormoor, K., Lawrence, D., Schlichting, L., Wilson, D., and Wong, W. K.: Evidence for changes in the magnitude and frequency of observed rainfall vs. snowmelt driven floods in Norway, Journal of Hydrology, 538, 33–48, 2016.

Wolff, M., Isaksen, K., Petersen-Øverleir, A., Ødemark, K., Reitan, T., and Brækkan, R.: Derivation of a new continuous adjustment function for correcting wind-induced loss of solid precipitation: results of a Norwegian field study, Hydrology and Earth System Sciences, 19, 951–967, 2015.

Earth Syst. Sci. Data Discuss., https://doi.org/10.5194/essd-2017-64
Manuscript under review for journal Earth Syst. Sci. Data
Discussion started: 28 August 2017

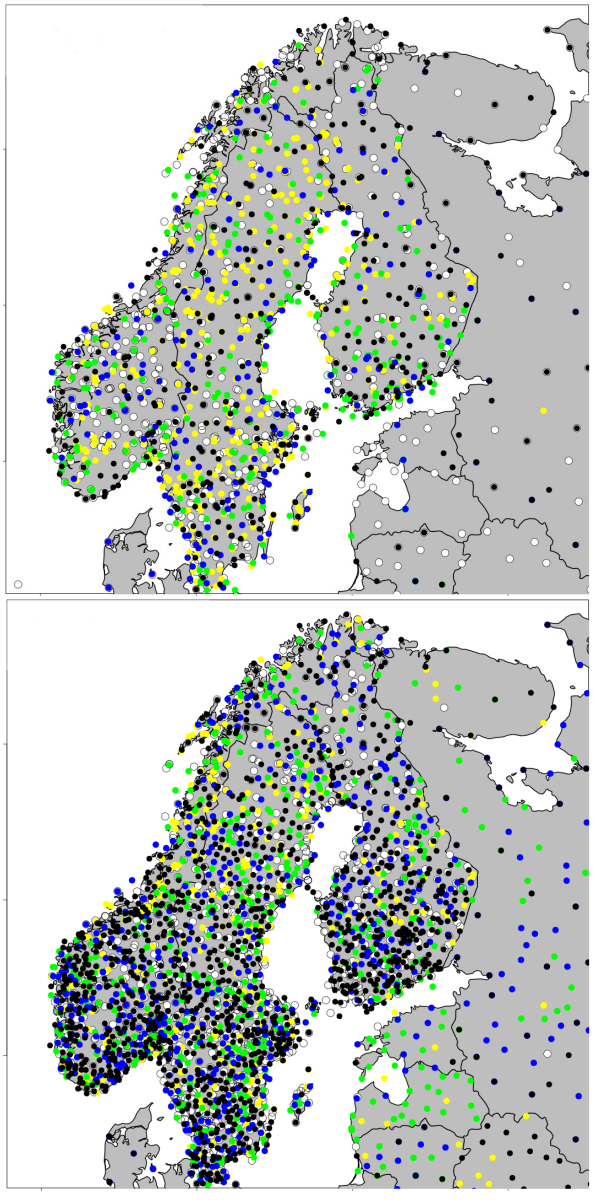

Figure 1. distribution of observation and percentage of data availability in the period 1971-2010. Top Panel: Daily averaged temperature. Bottom panel: daily total precipitation amount. The dots mark station locations and the color indicates the percentage of data available in the period: white $< 20\%$; yellow $< 40\%$; green $< 60\%$; blue $< 80\%$; black $\geq 80\%$

Earth Syst. Sci. Data Discuss., https://doi.org/10.5194/essd-2017-64
Manuscript under review for journal Earth Syst. Sci. Data
Discussion started: 28 August 2017

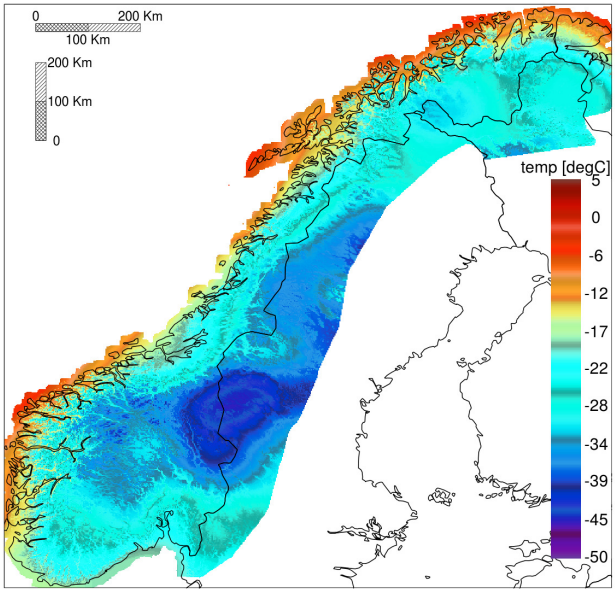

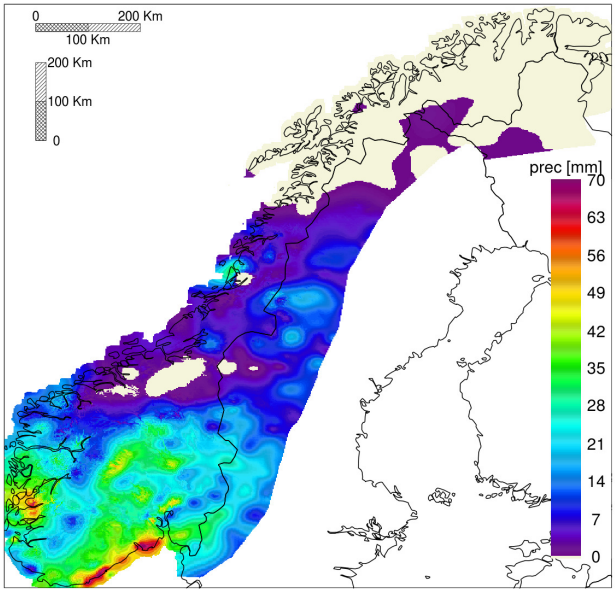

Figure 2. Examples of seNorge2 gridded fields. Top panel: Daily averaged temperature, 11 January 1987. Bottom panel: daily total precipitation amount, 24 November 2014.

Earth Syst. Sci. Data Discuss., https://doi.org/10.5194/essd-2017-64
Manuscript under review for journal Earth Syst. Sci. Data
Discussion started: 28 August 2017

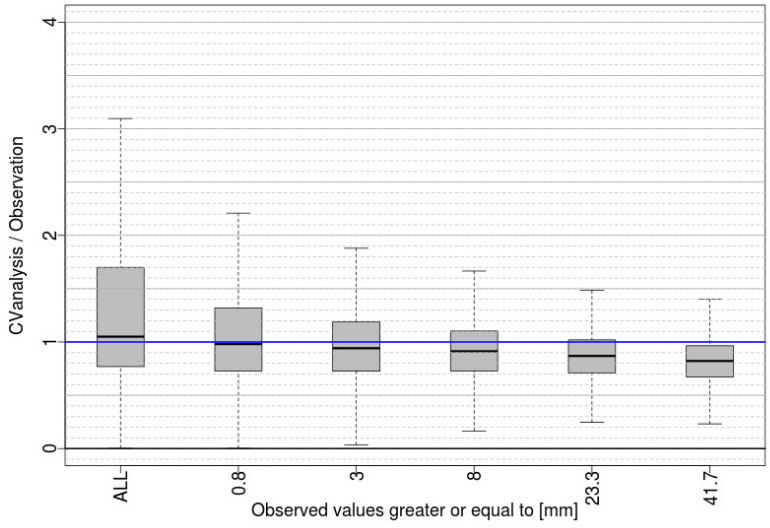

Figure 3. distribution of the relative error rel for daily precipitation (Eq. (10)) as a function of the precipitation intensity class. The distribution is represented by means of box-plots and each intensity class includes observations greater or equal to the value of its label. Time interval considered: 11 years, from 1 September 2003 to 31 August 2014.

Earth Syst. Sci. Data Discuss., https://doi.org/10.5194/essd-2017-64
Manuscript under review for journal Earth Syst. Sci. Data
Discussion started: 28 August 2017

Open Access Earth System Science Data Discussions

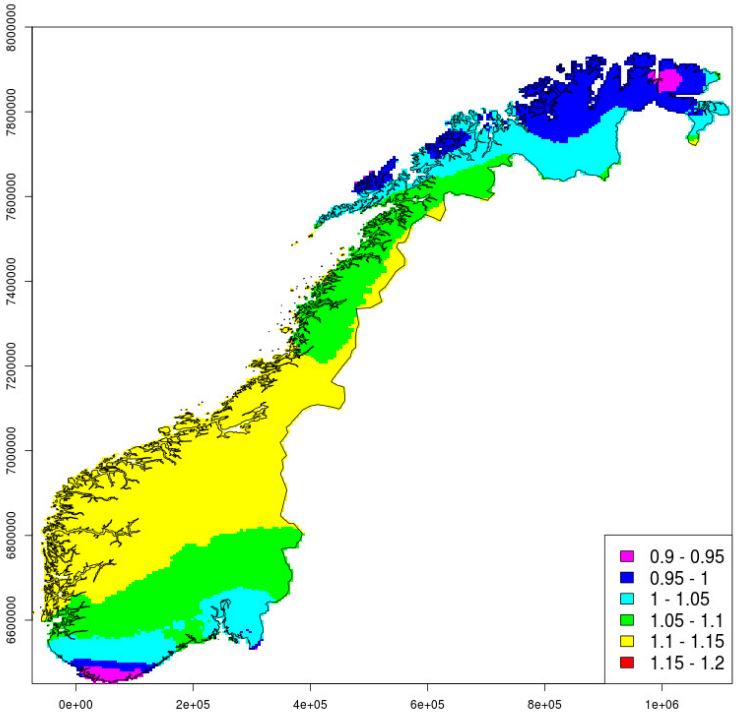

Figure 4. Daily precipitation. Spatial distribution for the mean value of $rel^{e}_{1.0\,\mathrm{mm}}$ (Eq. (11)). Time interval considered: 11 years, from 1 September 2003 to 31 August 2014.

Earth Syst. Sci. Data Discuss., https://doi.org/10.5194/essd-2017-64
Manuscript under review for journal Earth Syst. Sci. Data
Discussion started: 28 August 2017

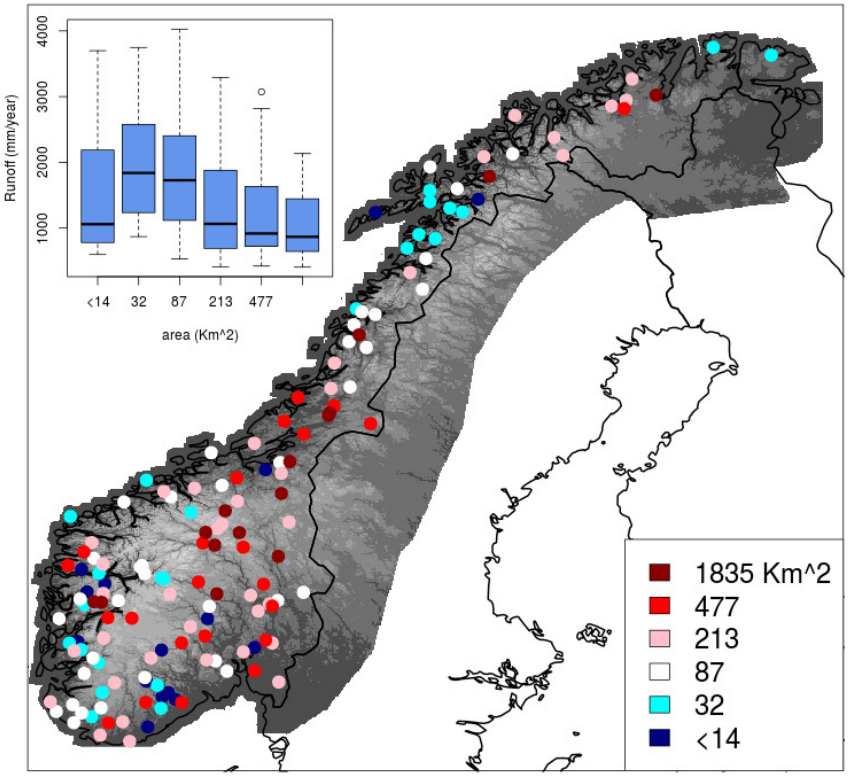

Figure 5. Sizes of Norwegian catchments without artificial influence and glaciers (area in Km^2). The box on the upper left corner shows the distributions of runoff for different catchment sizes.

Earth Syst. Sci. Data Discuss., https://doi.org/10.5194/essd-2017-64
Manuscript under review for journal Earth Syst. Sci. Data
Discussion started: 28 August 2017

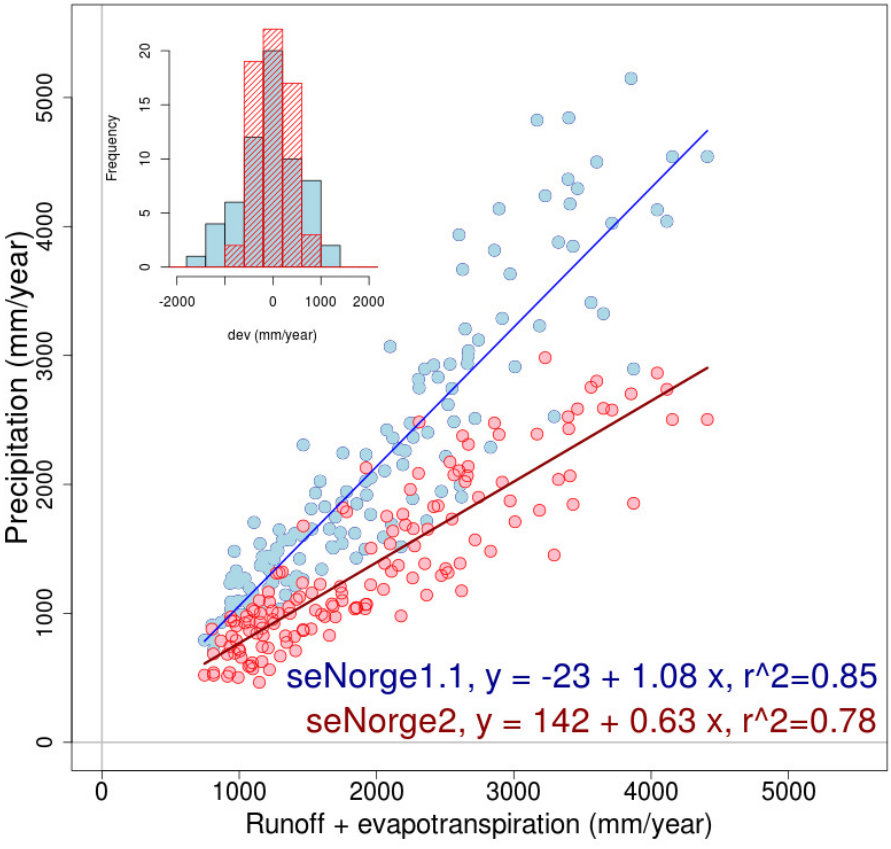

Figure 6. Average yearly precipitation (inputs of water to the catchment) against the sum of average yearly runoff and actual evapotranspiration (losses of water from the catchment) for the period from 1 January 2000 to 31 December 2013 for: seNorge1.1 (blue); seNorge2 (red). The upper left box shows the distribution of regression residuals when the sum of runoff and actual evapotranspiration exceeds 2000 mm/year.

Earth Syst. Sci. Data Discuss., https://doi.org/10.5194/essd-2017-64
Manuscript under review for journal Earth Syst. Sci. Data
Discussion started: 28 August 2017

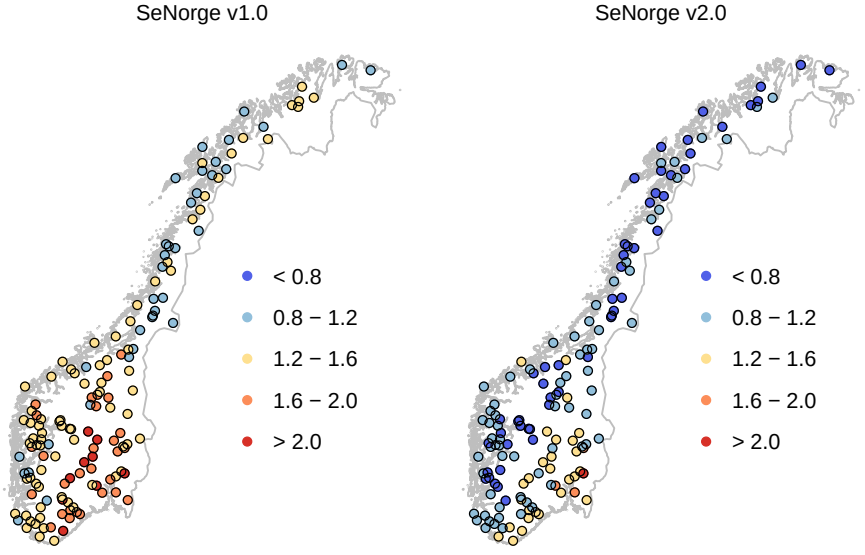

Figure 7. Ratio between total accumulated precipitation and runoff for the period from 1 January 2000 to 31 December 2013 for the two different seNorge versions.

Earth Syst. Sci. Data Discuss., https://doi.org/10.5194/essd-2017-64
Manuscript under review for journal Earth Syst. Sci. Data
Discussion started: 28 August 2017

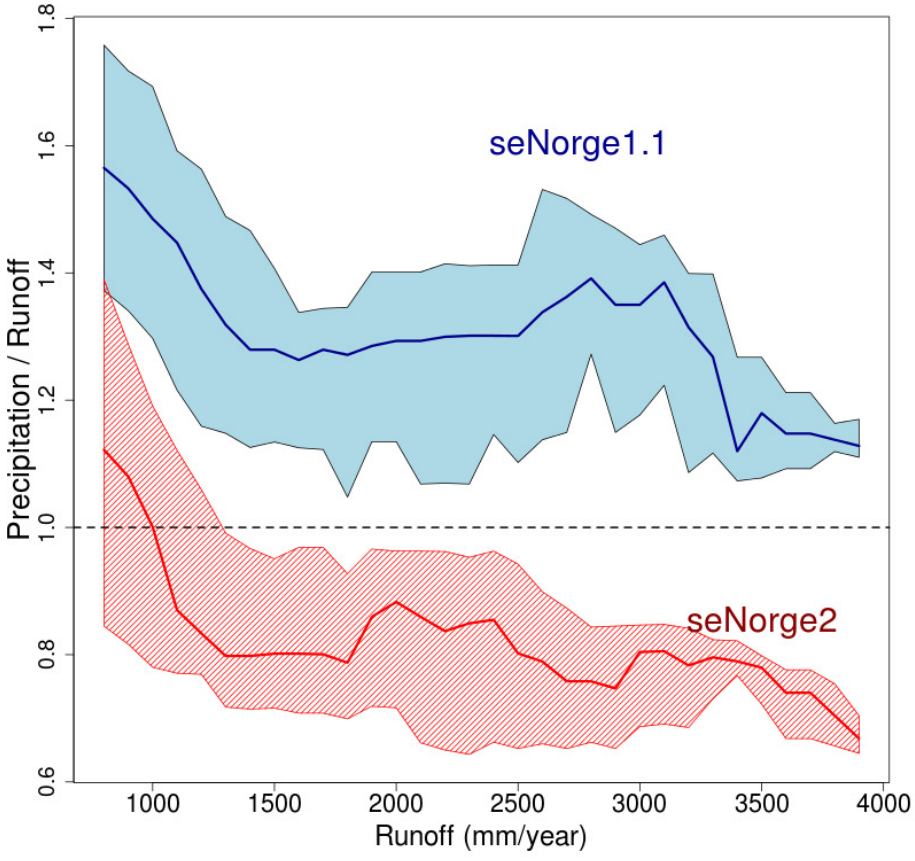

Figure 8. Ratio between total accumulated precipitation and runoff as a function of runoff. The original data is the same displayed in Figure 7. Each runoff value on the abscissa is a "label" of a class of runoff values centered around that value ($\pm$300mm/year). The thick line is the median of the distribution; the shaded area shows the interquartile range (i.e. difference between the third and the first quartile of the distribution of values). The number of catchments for each runoff class is the same as reported in the in-box of Figure 10.

Earth Syst. Sci. Data Discuss., https://doi.org/10.5194/essd-2017-64
Manuscript under review for journal Earth Syst. Sci. Data
Discussion started: 28 August 2017

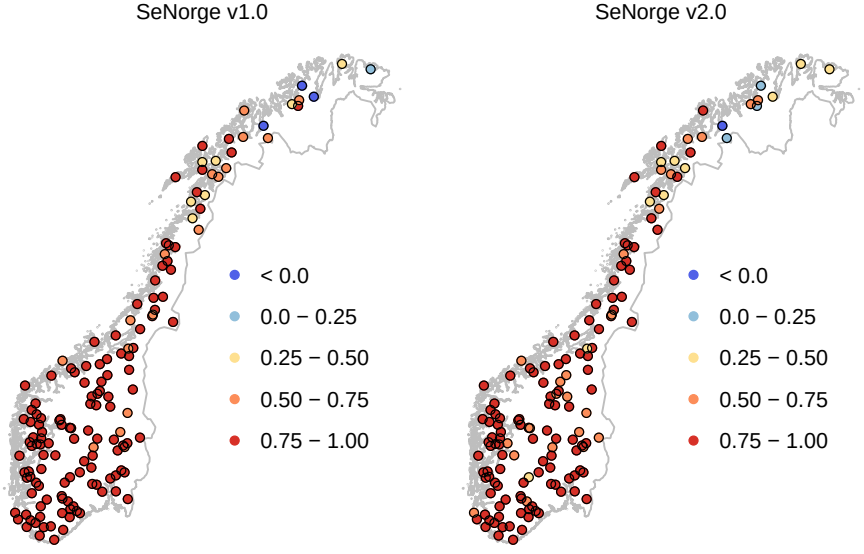

Figure 9. Correlation coefficient between yearly total precipitation and runoff for the period stretching from 1 January 2000 to 31 December 2013 for the two different seNorge versions.

Earth Syst. Sci. Data Discuss., https://doi.org/10.5194/essd-2017-64
Manuscript under review for journal Earth Syst. Sci. Data
Discussion started: 28 August 2017

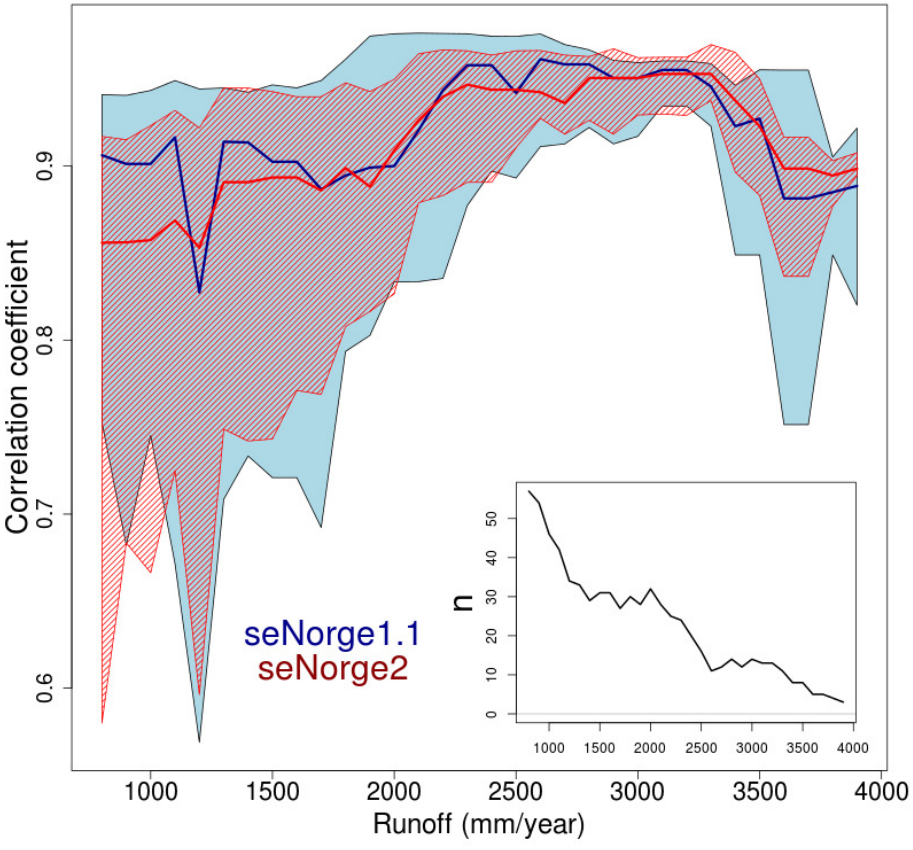

Figure 10. Correlation coefficient between yearly total precipitation and runoff as a function of runoff. The original data is the same displayed in Figure 9 and the format is the same as Figure 8. The in-box shows the number of catchments for each runoff threshold.

Earth Syst. Sci. Data Discuss., https://doi.org/10.5194/essd-2017-64
Manuscript under review for journal Earth Syst. Sci. Data
Discussion started: 28 August 2017

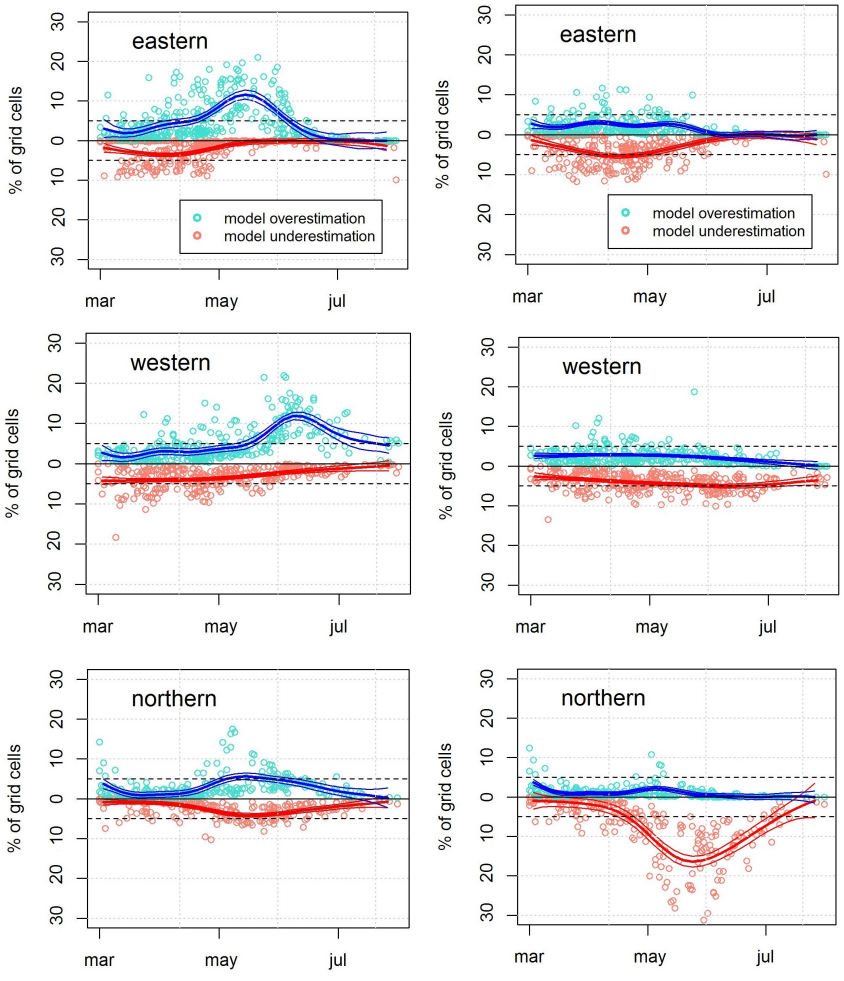

Figure 11. The model under- (F_u, red circles) and overestimation (F_o, blue circles) areas of SCA (% of all grid cells) in the three regions (Fig. 12) and for the two grid data versions (v.1.1. on the left column and v.2 on the right column) in 2001-2015 (in the days when a MODIS satellite image is available for comparison). The solid lines denote GAM-curves (with standard error) fitted to the cloud of points. The horizontal dashed lines denote the 5% deviation level within which the model results are considered as "good" in NVEs operational snow mapping (Saloranta, 2016).

Earth Syst. Sci. Data Discuss., https://doi.org/10.5194/essd-2017-64
Manuscript under review for journal Earth Syst. Sci. Data
Discussion started: 28 August 2017

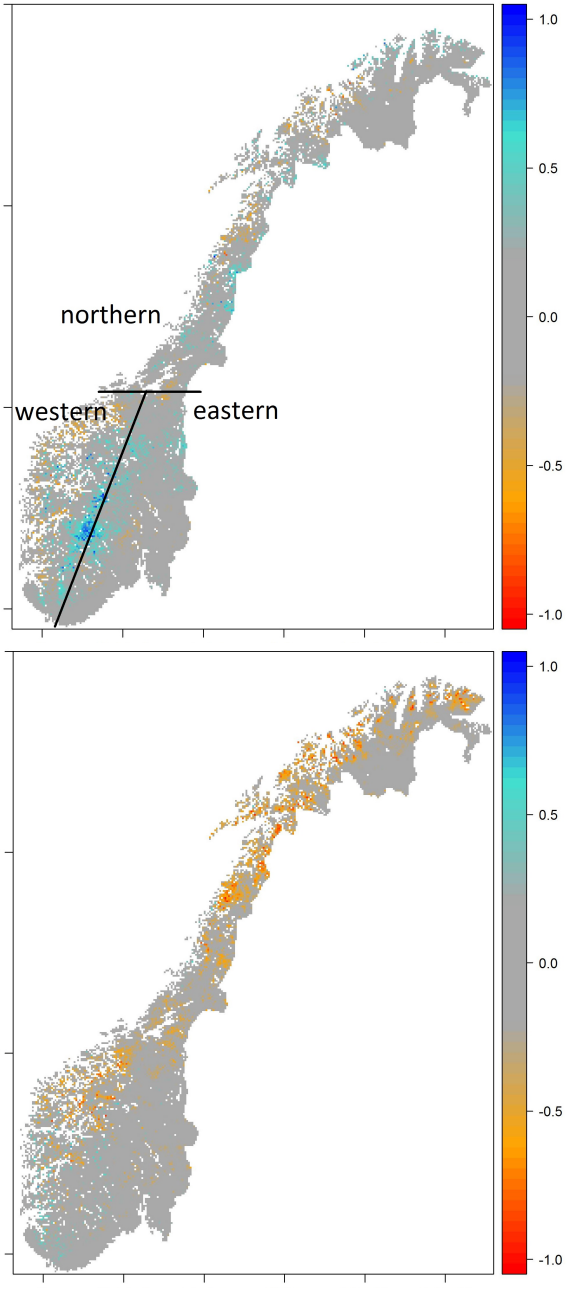

Figure 12. The bias index B for SCA in the seNorge grid cells for the two gridded dataset versions (v.1.1. on the top panel and v.2 on the bottom panel) in March-July 2001-2015. in the top panel, the three regions used in Figure. 11 are shown.

Earth Syst. Sci. Data Discuss., https://doi.org/10.5194/essd-2017-64
Manuscript under review for journal Earth Syst. Sci. Data
Discussion started: 28 August 2017

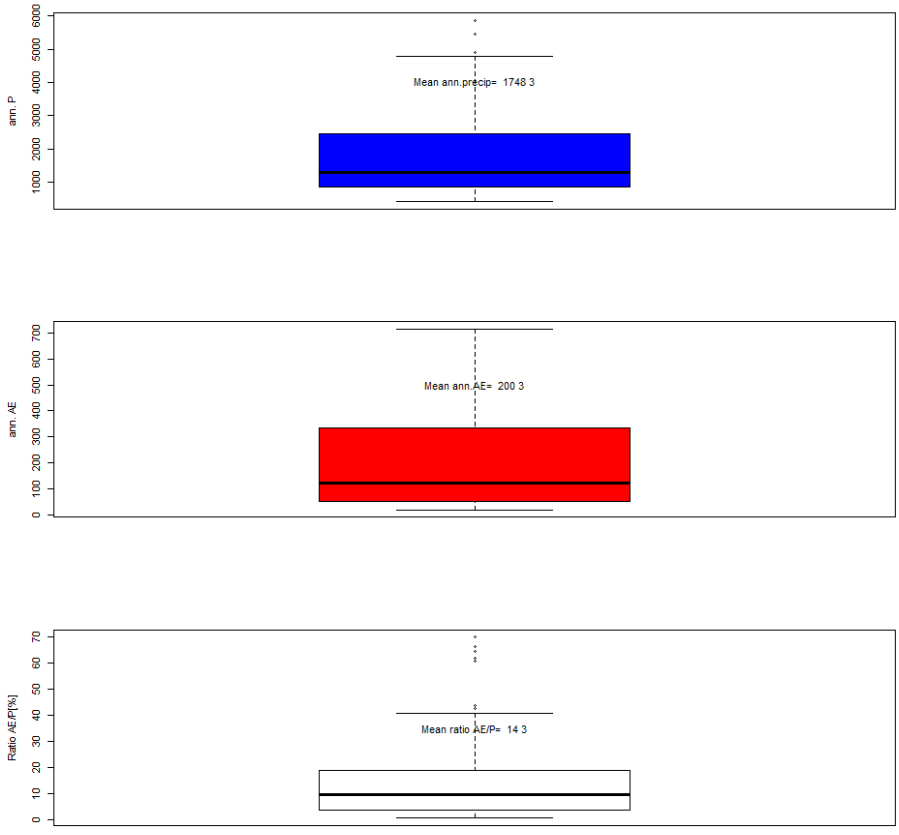

Figure 13. Boxplot of simulated precipitation (P) for 136 catchments (precipitation from seNorge 2.0 multiplied with P_{corr}) (top), simulated actual evapotranspiration (AE) (middle) and ratio between AE and P (bottom). Mean values are cited in the figures.

Earth Syst. Sci. Data Discuss., https://doi.org/10.5194/essd-2017-64
Manuscript under review for journal Earth Syst. Sci. Data
Discussion started: 28 August 2017

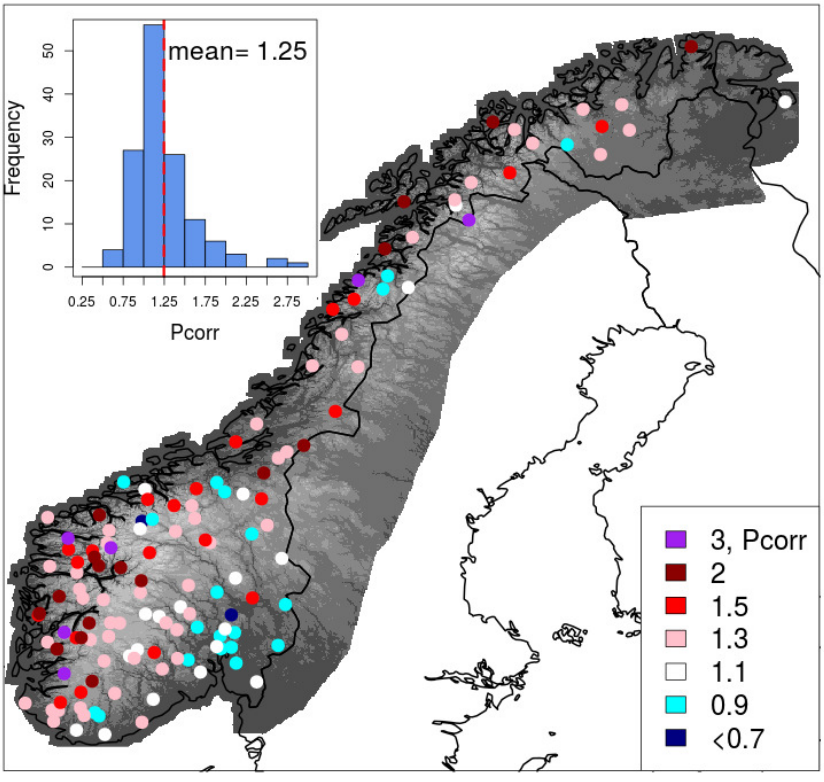

Figure 14. Geographical distribution of P_{corr}. The in-box shows the histograms with the distribution of P_{corr} values, the mean value is reported.

Earth Syst. Sci. Data Discuss., https://doi.org/10.5194/essd-2017-64
Manuscript under review for journal Earth Syst. Sci. Data
Discussion started: 28 August 2017

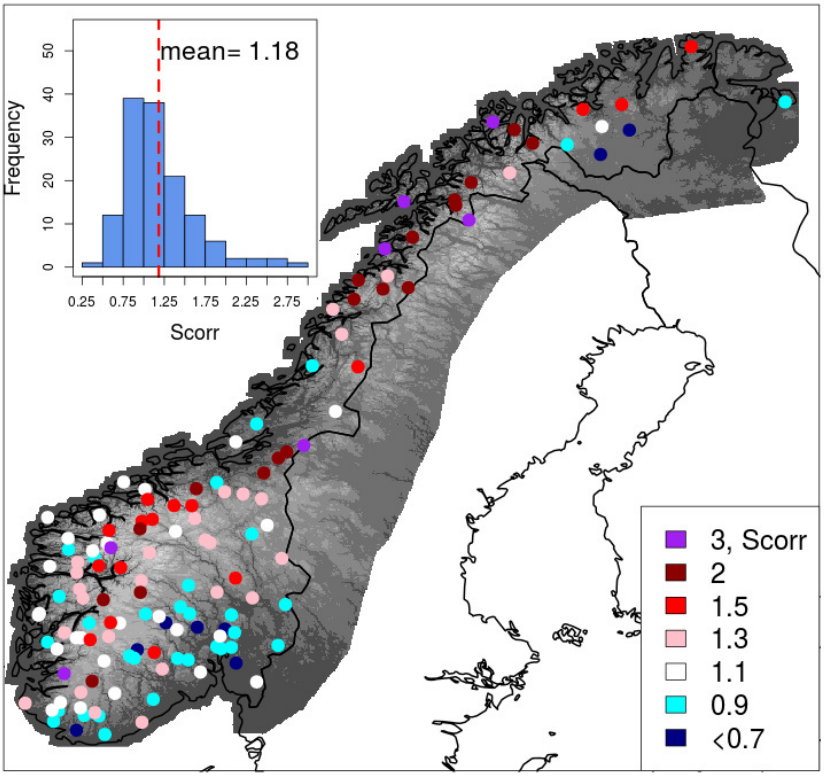

Figure 15. Geographical distribution of S_{corr}. The in-box shows the histograms with the distribution of S_{corr} values, the mean value is reported.